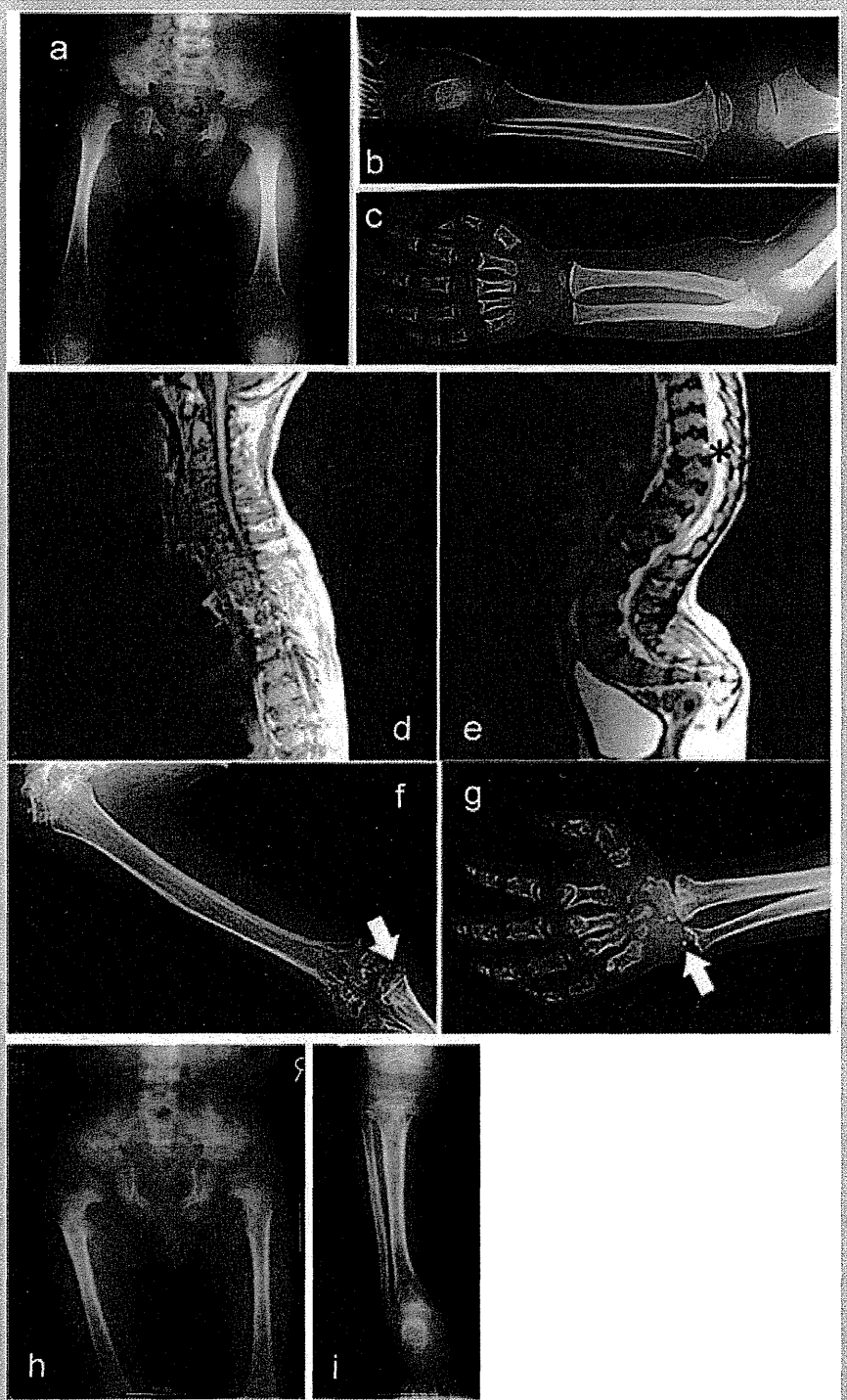

FIG. 2. Four years of age (a–c): (a) In the pelvis, upper acetabular margins are convexed and femoral heads are flattened. b: Metaphyses of Proximal tibia and distal femur are wide and flattened. The deformity of metaphyses is severer in upper limbs than lower ones. c: Proximal radius and ulnae are flared and broad. The appearances of epiphyses are delayed. 11 years of age (d–i): In the thoracic (d) and lumbar (e) spine, MRI of the spine shows flat and deformed vertebrae with wide and irregular intervertebral spaces. Lordosis is present. The spinal canal has enough space, and there is no spinal cord compression. f: The humerus is curved and shows radiolucency; and the distal end of metaphysis is broad and flared. Ossification of the epiphysis of the humerus is delayed for the age of 11 years and that of the ulna is absent (arrow). In (g), the metaphyses of both the radius and ulna are broad and flared at their distal ends. Stippled calcification is present in the distal end of the ulna. The epiphysis of the radius is present with soft tissue calcification around it. Small carpal bones are retarded in growth for the age of the patient. Metacarpal bones are short, the distal ends of metaphyses are broad, and the epiphyses are retarded for his age. The phalanges are short with corn-shaped epiphyses. h: In the pelvis, upper acetabular margins are convexed and femoral heads are flattened. The Ischia is short. i: Lower limbs. The distal femoral and proximal tibial metaphysis are wide and flattened. Stippled calcification is present on the epiphysis of proximal tibial bone.

TABLE I. Skeletal Survey of the Case of Neubauer et al. [2006] and of the Present Case

	Neubauer's case[a]	Present case
Tracheomalacia	−	+
Vertebrae		
Scoliosis	−	+
Flattened	+	+
Metaphyses		
Radiolucency	+	+
Deformity	+	+
Epiphyses		
Delay of appearance	−	+
Calcification	−	+
Tubular bones		
Short and deformed	−	+

[a]Case IV-9 (11-year-old male) reported by Neubauer et al. [2006].

intellectual disability have similar skeletal abnormality as our case, although our case has no lace-like appearance on pelvis X-ray which is the diagnostic abnormality of the former and the both have no signs of hypomyelination [Bieganski et al., 1999; Aglan et al., 2009]. Furthermore, the lethal syndrome of skeletal dysplasia and progressive central nervous system degeneration is different from our patient in its clinical course with death in early infancy [Khosravi et al., 1998].

To the best of our knowledge, this is the first patient documenting the coexistence of spondylo-meta-epiphyseal dysplasia and leukoencephalopathy. Since both spondylo-epi-metaphyseal dysplasia with short limb-hand type and central hypomyelination are rare conditions, and there is no mutation on the candidate genes of both diseases, it is appropriate to propose the possibility of a point mutation of unknown gene or promoter area rather than a contiguous gene syndrome judging from no causal CNVs recognized by CGH. Therefore, this case may indicate the presence of deficiency of an unidentified molecule crucial to both myelination and bone metabolism.

ACKNOWLEDGMENTS

We thank Dr. Gen Nishimura for his help in the diagnosis of skeletal dysplasia.

REFERENCES

Aglan MS, Temtamy SA, Fateen E, Ashour AM, Eldeeb K, Hosny GA. 2009. Dyggve–Melchior–Clausen syndrome: Clinical, genetic, and radiological study of 15 Egyptian patients from nine unrelated families. J Child Orthop 3:451–458.

al-Gazali LI, Bakalinova D, Sztriha L. 1996. Spondylo-meta-epiphyseal dysplasia, short limb, abnormal calcification type. Clin Dysmorphol 5:197–206.

Bargal R, Cormier-Daire V, Ben-Neriah Z, Le Merrer M, Sosna J, Melki J, Zangen DH, Smithson SF, Borochowitz Z, Belostotsky R, Raas-Rothschild A. 2009. Mutations in DDR2 gene cause SMED with short limbs and abnormal calcifications. Am J Hum Genet 84:80–84.

Bieganski T, Dawydzik B, Kozlowski K. 1999. Spondylo-epimetaphyseal dysplasia: A new X-linked variant with mental retardation. Eur J Pediatr 158:809–814.

Cormier-Daire V. 2008. Spondylo-epi-metaphyseal dysplasia. Best Pract Res Clin Rheumatol 22:33–44.

Deguchi K, Clewing JM, Elizondo LI, Hirano R, Huang C, Choi K, Sloan EA, Lucke T, Marwedel KM, Powell RD Jr, Santa Cruz K, Willaime-Morawek S, Inoue K, Lou S, Northrop JL, Kanemura Y, van der Kooy D, Okano H, Armstrong DL, Boerkoel CF. 2008. Neurologic phenotype of Schimke immuno-osseous dysplasia and neurodevelopmental expression of SMARCAL1. J Neuropathol Exp Neurol 67: 565–577.

Inoue K, Osaka H, Imaizumi K, Nezu A, Takanashi J, Arii J, Murayama K, Ono J, Kikawa Y, Mito T, Shaffer LG, Lupski JR. 1999. Proteolipid protein gene duplications causing Pelizaeus–Merzbacher disease: Molecular mechanism and phenotypic manifestations. Ann Neurol 45:624–632.

Kagitani K, Fukunishi M, Mano T, Matsuoka T, Imai K, Ono J, Okada S. 1999. Connatal type of Pelizaeus–Merzbacher disease: A case report. No To Hattatsu 31:171–176.

Khosravi M, Weaver DD, Bull MJ, Lachman R, Rimoin DL. 1998. Lethal syndrome of skeletal dysplasia and progressive central nervous system degeneration. Am J Med Genet 77:63–71.

Lazzarini RA, Griffin JW, Lassman H, Nave K-A, Miller R, Trapp BD, editors. 2004. Pelizaeus–Merzbache disease. Myelin biology and disorders, 2nd edition, Volume 2, Chapter 37. USA: Elsevier. pp 867–881.

Miyake N, Shimokawa O, Harada N, Sosonkina N, Okubo A, Kawara H, Okamoto N, Kurosawa K, Kawame H, Iwakoshi M, Kosho T, Fukushima Y, Makita Y, Yokoyama Y, Yamagata T, Kato M, Hiraki Y, Nomura M, Yoshiura K, Kishino T, Ohta T, Mizuguchi T, Niikawa N, Matsumoto N. 2006. BAC array CGH reveals genomic aberrations in idiopathic mental retardation. Am J Med Genet Part A 140A:205–211.

Neubauer BA, Stefanova I, Hubner CA, Neumaier-Probst E, Bohl J, Oppermann HC, Sto H, Hahn A, Stephani U, Kohlschutter A, Gal A. 2006. A new type of leukoencephalopathy with metaphyseal chondrodysplasia maps to Xq25–q27. Neurology 67:587–591.

Osaka H, Kawanishi C, Inoue K, Onishi H, Kobayashi T, Sugiyama N, Kosaka K, Nezu A, Fujii K, Sugita K, Kodama K, Murayama K, Murayama S, Kanazawa I, Kimura S. 1999. Pelizaeus–Merzbacher disease: Three novel mutations and implication for locus heterogeneity. Ann Neurol 45:59–64.

Powers JM. 2004. The leukodystrophies: Overview and classification, myelin biology and disorders, 2nd edition, Volume 2, Chapter 28. USA: Elsevier. pp 663–690.

Renella R, Schaefer E, LeMerrer M, Alanay Y, Kandemir N, Eich G, Costa T, Ballhausen D, Boltshauser E, Bonafe L, Giedion A, Unger S, Superti-Furga A. 2006. Spondyloenchondrodysplasia with spasticity, cerebral calcifications, and immune dysregulation: Clinical and radiographic delineation of a pleiotropic disorder. Am J Med Genet Part A 140A:541–550.

van der Knaap MS, Naidu S, Pouwels PJ, Bonavita S, van Coster R, Lagae L, Sperner J, Surtees R, Schiffmann R, Valk J. 2002. New syndrome characterized by hypomyelination with atrophy of the basal ganglia and cerebellum. Am J Neuroradiol 23:1466–1474.

nature genetics

Mutations affecting components of the SWI/SNF complex cause Coffin-Siris syndrome

Yoshinori Tsurusaki[1], Nobuhiko Okamoto[2], Hirofumi Ohashi[3], Tomoki Kosho[4], Yoko Imai[5], Yumiko Hibi-Ko[5], Tadashi Kaname[6], Kenji Naritomi[6], Hiroshi Kawame[7,8], Keiko Wakui[4], Yoshimitsu Fukushima[4], Tomomi Homma[9], Mitsuhiro Kato[10], Yoko Hiraki[11], Takanori Yamagata[12], Shoji Yano[13], Seiji Mizuno[14], Satoru Sakazume[15], Takuma Ishii[15,16], Toshiro Nagai[15], Masaaki Shiina[17], Kazuhiro Ogata[17], Tohru Ohta[18], Norio Niikawa[18], Satoko Miyatake[1], Ippei Okada[1], Takeshi Mizuguchi[1], Hiroshi Doi[1], Hirotomo Saitsu[1], Noriko Miyake[1] & Naomichi Matsumoto[1]

By exome sequencing, we found *de novo SMARCB1* mutations in two of five individuals with typical Coffin-Siris syndrome (CSS), a rare autosomal dominant anomaly syndrome. As *SMARCB1* encodes a subunit of the SWItch/Sucrose NonFermenting (SWI/SNF) complex, we screened 15 other genes encoding subunits of this complex in 23 individuals with CSS. Twenty affected individuals (87%) each had a germline mutation in one of six SWI/SNF subunit genes, including *SMARCB1*, *SMARCA4*, *SMARCA2*, *SMARCE1*, *ARID1A* and *ARID1B*.

Chromatin remodeling factors regulate the gene accessibility and expression by dynamic alteration of chromatin structure. SWI/SNF complexes have important roles in lineage specification, maintenance of stem cell pluripotency and tumorigenesis[1–5]. These complexes are composed of evolutionarily conserved core subunits and variant subunits. Brahma-associated factor (BAF) and Polybromo BAF (PBAF) complexes constitute two major subclasses[1–5]. It has been suggested that the BAF complex is similar to the yeast SWI/SNF complex and that the PBAF complex is more like the chromatin remodelling complex (RSC) in yeast, which is required for cell cycle progression through mitosis[6]. However, several subunits that are common to both BAF and PBAF complexes are predicted to be related to the regulation of lineage- and tissue-specific gene expression[2].

Coffin-Siris syndrome (MIM 135900) is a rare congenital anomaly syndrome characterized by growth deficiency, intellectual disability, microcephaly, coarse facial features and hypoplastic nail of the fifth finger and/or toe (**Fig. 1** and **Supplementary Table 1**)[7]. The majority of affected individuals represent sporadic cases, which is compatible with an autosomal dominant inheritance mechanism. The genetic cause for this syndrome has not been elucidated.

To identify the genetic basis of CSS, we performed whole-exome sequencing of five typical affected individuals (**Supplementary Methods**). Taking into account our model that assumes that an abnormality in a causal gene would be shared in two or more subjects, 51 variants were identified as candidates (**Supplementary Table 2**). All the variants were also examined by Sanger sequencing of PCR products amplified using genomic DNA from the five affected individuals and their parents. Nine variants were found to be false positives, 40 were inherited from either the father or mother, and 2 *de novo* heterozygous mutations of *SMARCB1* were found in 2 affected individuals (c.1130G>A (p.Arg377His) and c.1091_1093del AGA (p.Lys364del)) (**Table 1**, **Supplementary Fig. 1** and **Supplementary Methods**). Two *de novo* coding-sequence mutations occurring within a specific gene is an extremely unlikely event[8], supporting the idea that *SMARCB1* is a causative gene in CSS. Next, we screened *SMARCB1* in 23 individuals with CSS by high-resolution melting analysis[9] and identified the mutation encoding the p.Lys364del alteration in two additional individuals, including one of Arab descent (subject 22) (**Table 1** and **Supplementary Fig. 1**). As the mutation detection rate was relatively low (4 of 23, only 17.4%), we screened 15 additional genes encoding other SWI/SNF subunits (**Supplementary Table 3**). Unexpectedly, four other subunits, *SMARCA4* (also known as *BRG1*), *SMARCE1*, *ARID1A* and *ARID1B* were also found to be mutated (**Table 1** and **Supplementary Figs. 2–5**). In subject 10, a, c.2144C>T mutation in *ARID1B* (encoding p.Pro715Leu) was found in addition to the c.5632delG mutation in *ARID1B*. RT-PCR products that were amplified from total RNA from this subject's lymphoblastoid cells were cloned into the pCR4-TOPO vector. The two mutations were present on different alleles, according to sequencing of clones containing each allele (data not shown). As the c.5632delG mutation is

[1]Department of Human Genetics, Yokohama City University Graduate School of Medicine, Yokohama, Japan. [2]Division of Medical Genetics, Osaka Medical Center and Research Institute for Maternal and Child Health, Izumi, Japan. [3]Division of Medical Genetics, Saitama Children's Medical Center, Iwatsuki, Japan. [4]Department of Medical Genetics, Shinshu University School of Medicine, Matsumoto, Japan. [5]Division of Pediatrics, Japanese Red Cross Medical Center, Tokyo, Japan. [6]Department of Medical Genetics, University of the Ryukyus Faculty of Medicine, Okinawa, Japan. [7]Department of Genetic Counseling, Graduate School of Humanities and Sciences, Ochanomizu University, Tokyo, Japan. [8]Division of Medical Genetics, Nagano Children's Hospital, Azumino, Japan. [9]Division of Pediatrics, Yamagata Prefectural and Sakata Municipal Hospital Organization, Nihonkai General Hospital, Sakata, Japan. [10]Department of Pediatrics, Yamagata University Faculty of Medicine, Yamagata, Japan. [11]Hiroshima Municipal Center for Child Health and Development, Hiroshima, Japan. [12]Department of Pediatrics, Jichi Medical University, Tochigi, Japan. [13]Genetics Division, Department of Pediatrics, Los Angeles County and University of Southern California Medical Center, Keck School of Medicine, University of Southern California, Los Angeles, California, USA. [14]Department of Pediatrics, Central Hospital, Aichi Human Service Center, Kasugai, Japan. [15]Department of Pediatrics, Koshigaya Hospital, Dokkyo University School of Medicine, Koshigaya, Japan. [16]Nakagawa-No-Sato, Hospital for the Disabled, Saitama, Japan. [17]Department of Biochemistry, Yokohama City University Graduate School of Medicine, Yokohama, Japan. [18]Research Institute of Personalized Health Sciences, Health Sciences University of Hokkaido, Ishikari-Tobetsu, Japan. Correspondence should be addressed to N. Matsumoto (naomat@yokohama-cu.ac.jp) or N. Miyake (nmiyake@yokohama-cu.ac.jp).

Received 29 September 2011; accepted 10 February 2012; published online 18 March 2012; doi:10.1038/ng.2219

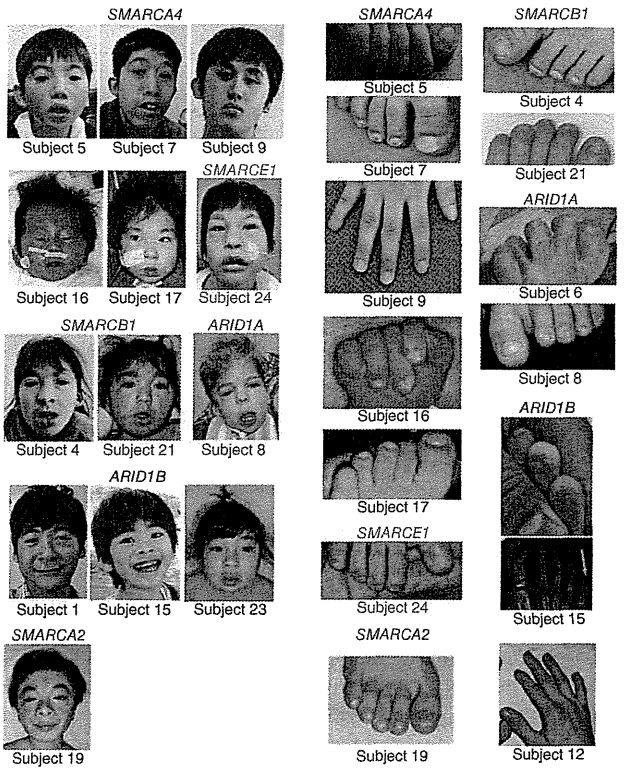

Figure 1 Photographs of individuals with Coffin-Siris syndrome. The faces (left) and hypoplastic-to-absent nail of the fifth finger or toe (right) of affected individuals are shown with the color-coded names of the corresponding mutated genes. The green arrow indicates the absence of the distal phalanx in the fifth toe. No obvious hypoplastic nails were observed in subjects 12 or 19. Consent for all the photographs was obtained from the families of the affected individuals.

very likely to be deleterious (as it results in a truncated protein), the c.2144C>T mutation is likely to be a rare polymorphism. Of note, subject 12, who presented an atypical facial appearance and indistinct hypoplastic nails, had two interstitial deletions at 6q25.3–q27 involving *ARID1B*, as detected by a SNP array (**Supplementary Fig. 6** and **Supplementary Methods**). Furthermore, subject 14 was found to have an interstitial deletion of *SMARCA2* by a SNP array (**Supplementary Fig. 7** and **Supplementary Methods**). No other copy-number changes involving genes encoding SWI/SNF complex components were found in subjects 2, 14 or 18 by array analysis. The overall mutation detection rate was 87%. In total, 20 of the 23 subjects had a mutation affecting one of the six SWI/SNF subunits.

Mutations in CSS were identified in the BAF-specific subunits *ARID1A* and *ARID1B* but not in PBAF-specific subunits (*BRD7*, *ARID2* and *PBRM1*) (**Supplementary Table 3**). In addition, mutations were identified in *SMARCA4* (*BRG1*) as well as in *SMARCA2* (*BRM*) (**Supplementary Table 3**). The BRG1 and BRM proteins are mutually exclusive catalytic ATP subunits in mammalian SWI/SNF complexes. Of note, the majority of heterozygous *Smarca4*-null mice survive with susceptibility to neoplasia, with a minority dying after birth because of exencephaly, whereas homozygous *Smarca2*-null mice are viable and fertile[4]. In *Smarca2*-null mice, Brg1 is upregulated, suggesting that Brg1 can functionally replace Brm in mice[10]. However, in humans, abnormalities in both *SMARCA4* and *SMARCA2* are found in CSS, indicating that the in-frame partial deletion of the gene encoding BRM in subject 19 has a specific mutational effect different from that of simple inactivation in mice. These data support the idea that abnormalities in the BRG1-BAF and BRM-BAF complexes can cause the abnormal neurological development in CSS.

All the mutated genes found in CSS, except for *SMARCE1*, have been reported to be associated with tumorigenesis[1,2]. Among the 23 subjects with CSS, only subject 3 with an *ARID1A* mutation presented with hepatoblastoma. To our knowledge, haploinsufficiency and/or homozygous inactivation of *ARID1A* have been found in several types of cancer but not in hepatoblastoma. Malignancies were not detected in any of the other subjects with CSS examined here. It remains to be seen whether malignancies are robustly associated with CSS.

Given the fact that all the mutations in *ARID1A* and *ARID1B* in CSS were predicted to cause protein truncation, we proposed that haploinsufficiency of these two genes must be able to cause CSS. cDNA analysis of lymphoblastoid cell lines from subjects 1, 6 and 23 indicated that the mutated transcripts were subject to nonsense-mediated mRNA decay (**Supplementary Fig. 8**). In subject 10, the *ARID1B* mutation associated with the creation of a premature stop codon in the last exon did not result in nonsense-mediated mRNA decay as expected (**Supplementary Fig. 8**).

In regard to the other mutated genes, germline heterozygous truncation mutations in *SMARCB1* and *SMARCA4* have been reported

Table 1 Mutations in individuals with Coffin-Siris syndrome

Subject ID	Gene	Mutation	Alteration	Type	Control allele frequency[a]
4	*SMARCB1*	c.1091_1093del AGA	p.Lys364del	*De novo*	0/502
11	*SMARCB1*	c.1130G>A	p.Arg377His	*De novo*	0/500
21	*SMARCB1*	c.1091_1093del AGA	p.Lys364del	NC	0/502
22	*SMARCB1*	c.1091_1093del AGA	p.Lys364del	NC	0/502
9	*SMARCA4*	c.1636_1638del AAG	p.Lys546del	*De novo*	0/350
7	*SMARCA4*	c.2576C>T	p.Thr859Met	*De novo*	0/368
5	*SMARCA4*	c.2653C>T	p.Arg885Cys	*De novo*	0/368
16	*SMARCA4*	c.2761C>T	p.Leu921Phe	*De novo*	0/368
25	*SMARCA4*	c.3032T>C	p.Met1011Thr	NC	0/372
17	*SMARCA4*	c.3469C>G	p.Arg1157Gly	*De novo*	0/368
19	*SMARCA2*	Partial deletion		*De novo*	–
24	*SMARCE1*	c.218A>G	p.Tyr73Cys	*De novo*	0/368
3	*ARID1A*	c.31_56del	p.Ser11Alafs*91	NC	0/330
6	*ARID1A*	c.2758C>T	p.Gln920*	NC	0/376
8	*ARID1A*	c.4003C>T	p.Arg1335*	*De novo*	–
1	*ARID1B*	c.1678_1688del	p.Ile560Glyfs*89	*De novo*	–
15	*ARID1B*	c.1903C>T	p.Gln635*	*De novo*	–
23	*ARID1B*	c.3304C>T	p.Arg1102*	*De novo*	–
10	*ARID1B*	c.2144C>T	p.Pro715Leu	NC	0/368
10	*ARID1B*	c.5632del G	p.Asp1878Metfs*96	NC	0/374
12	*ARID1B*	Microdeletion		NC	–

NC, not confirmed because parental samples were unavailable.
[a]The numbers indicate the observed allele frequency (alleles harboring the change/total tested alleles) in Japanese controls. None of the mutations was found in dbSNP132, the 1000 Genomes database or the National Heart, Lung, and Blood Institute (NHLBI) GO exomesequencing project database. –, not tested.

in individuals with rhabdoid tumor predisposition syndromes 1 (RTPS1; MIM 609322) and 2 (RTPS2; MIM 613325)[11,12], and various types of *SMARCB1* mutations (missense, in-frame deletion, nonsense and splice site) have been found in the germline of individuals with familial and sporadic schwannomatosis (MIM 162091)[13,14]. Furthermore, mice with heterozygous knockout of *Smarca4* or *Smarcb1* were prone to tumor development[2]. All the mutations in *SMARCA4* and *SMARCB1* in individuals with CSS were nontruncating (either missense or in-frame deletions), implying that they exert gain-of-function or dominant-negative effects (excluding haploinsufficiency as a cause). It is noteworthy that comparable germline mutations in *SMARCB1* have such different phenotypic consequences in their association with the phenotypes of CSS and schwannomatosis. The *SMARCB1* mutations in CSS and those in schwannomatosis are indeed different according to the Human Gene Mutation Database. With regard to the *SMARCA2* interstitial deletion in CSS, the change maintained the coding sequence reading frame but removed exons 20–27 that encode the HELICc domain. RT-PCR analysis confirmed the deletion of exons 20–27 at the cDNA level (**Supplementary Fig. 7**). These data suggest the importance of the HELICc domain in the SMARCA2 protein.

The various types of mutations in the genes encoding different SWI/SNF components resulted in similar CSS phenotypes. This suggests that the SWI/SNF complexes coordinately regulate chromatin structure and gene expression. This is the first report, to our knowledge, of germline mutations in SWI/SNF complex genes associated with a multiple congenital anomaly syndrome, highlighting new biological aspects of SWI/SNF complexes in humans. Similarly, genes encoding SNF2-related proteins, which are implicated as chromatin remodeling factors outside of SWI/SNF complexes, are mutated in different syndromes, including in α-thalassaemia/mental retardation syndrome X-linked (ATRX; *ATRX* mutations) and in coloboma, heart defect, atresia choanae, retarded growth and development, genital abnormality and ear abnormality (CHARGE) syndrome (*CHD7* haploinsufficiency)[3]. We expect that more mutations affecting chromatin remodeling factors will be found in different human diseases.

URLs. Human Gene Mutation Database, https://portal.biobase-international.com/cgi-bin/portal/login.cgi.

Note: Supplementary information is available on the Nature Genetics website.

ACKNOWLEDGMENTS

We thank all the family members for participating in this study. This work was supported by research grants from the Ministry of Health, Labour and Welfare (to N. Miyake, H.S. and N. Matsumoto), the Japan Science and Technology Agency (to N. Matsumoto), the Strategic Research Program for Brain Sciences (to N. Matsumoto), the Japan Epilepsy Research Foundation (to H.S.) and the Takeda Science Foundation (to N. Matsumoto and N. Miyake). This study was also funded by a Grant-in-Aid for Scientific Research on Innovative Areas (Foundation of Synapse and Neurocircuit Pathology) from the Ministry of Education, Culture, Sports, Science and Technology of Japan (to N. Matsumoto), a Grant-in-Aid for Scientific Research from the Japan Society for the Promotion of Science (to N. Matsumoto), a Grant-in-Aid for Young Scientists from the Japan Society for the Promotion of Science (to N. Miyake and H.S.) and a Grant for 2011 Strategic Research Promotion of Yokohama City University (to N. Matsumoto). This study was performed at the Advanced Medical Research Center at Yokohama City University. Informed consent was obtained from all the families of affected individuals. The Institutional Review Board of Yokohama City University approved this study.

AUTHOR CONTRIBUTIONS

Y.T., S. Miyatake, I.O., H.D., H.S. and N. Miyake performed exome sequencing and Sanger sequencing. Y.T., M.S., K.O., I.O., T.M., H.D., H.S. and N. Miyake performed data management and analysis. N.O., H.O., T. Kosho, Y.I., Y.H.-K., T. Kaname, K.N., H.K., K.W., Y.F., T.H., M.K., Y.H., T.Y., S.Y., S. Mizuno, S.S., T.I., T.N., T.O. and N.N. provided clinical materials after careful evaluation. Y.T., N. Miyake and N. Matsumoto wrote the manuscript. N. Matsumoto designed and oversaw all aspects of the study.

COMPETING FINANCIAL INTERESTS

The authors declare no competing financial interests.

Published online at http://www.nature.com/naturegenetics/.
Reprints and permissions information is available online at http://www.nature.com/reprints/index.html.

1. Reisman, D., Glaros, S. & Thompson, E.A. *Oncogene* **28**, 1653–1668 (2009).
2. Wilson, B.G. & Roberts, C.W. *Nat. Rev. Cancer* **11**, 481–492 (2011).
3. Clapier, C.R. & Cairns, B.R. *Annu. Rev. Biochem.* **78**, 273–304 (2009).
4. Bultman, S. *et al. Mol. Cell* **6**, 1287–1295 (2000).
5. Hargreaves, D.C. & Crabtree, G.R. *Cell Res.* **21**, 396–420 (2011).
6. Xue, Y. *et al. Proc. Natl. Acad. Sci. USA* **97**, 13015–13020 (2000).
7. Coffin, G.S. & Siris, E. *Am. J. Dis. Child.* **119**, 433–439 (1970).
8. Bamshad, M.J. *et al. Nat. Rev. Genet.* **12**, 745–755 (2011).
9. Wittwer, C.T., Reed, G.H., Gundry, C.N., Vandersteen, J.G. & Pryor, R.J. *Clin. Chem.* **49**, 853–860 (2003).
10. Reyes, J.C. *et al. EMBO J.* **17**, 6979–6991 (1998).
11. Schneppenheim, R. *et al. Am. J. Hum. Genet.* **86**, 279–284 (2010).
12. Taylor, M.D. *et al. Am. J. Hum. Genet.* **66**, 1403–1406 (2000).
13. Boyd, C. *et al. Clin. Genet.* **74**, 358–366 (2008).
14. Hadfield, K.D. *et al. J. Med. Genet.* **45**, 332–339 (2008).

ORIGINAL ARTICLE

PAPSS2 mutations cause autosomal recessive brachyolmia

Noriko Miyake,[1] Nursel H Elcioglu,[2] Aritoshi Iida,[3] Pinar Isguven,[4] Jin Dai,[3] Nobuyuki Murakami,[5] Kazuyuki Takamura,[6] Tae-Joon Cho,[7] Ok-Hwa Kim,[8] Tomonobu Hasegawa,[9] Toshiro Nagai,[5] Hirofumi Ohashi,[10] Gen Nishimura,[11] Naomichi Matsumoto,[1] Shiro Ikegawa[3]

[1]Department of Human Genetics, Yokohama City University Graduate School of Medicine, Yokohama, Japan
[2]Department of Pediatric Genetics, Marmara University Pendik Hospital, Istanbul, Turkey
[3]Laboratory for Bone and Joint Diseases, Center for Genomic Medicine, RIKEN, Tokyo, Japan
[4]Department of Pediatrics and Pediatric Endocrinology, Medeniyet University Goztepe Hospital, Istanbul, Turkey
[5]Department of Pediatrics, Dokkyo Medical University Koshigaya Hospital, Koshigaya, Japan
[6]Department of Orthopaedic Surgery, Fukuoka Children's Hospital, Fukuoka, Japan
[7]Division of Pediatric Orthopaedics, Seoul National University Children's Hospital, Seoul, Korea
[8]Department of Radiology, Ajou University Hospital, Suwon, Korea
[9]Department of Pediatrics, Keio University School of Medicine, Tokyo, Japan
[10]Division of Medical Genetics, Saitama Children's Medical Center, Saitama, Japan
[11]Department of Pediatric Imaging, Tokyo Metropolitan Children's Medical Center, Futyu, Japan

Correspondence to
Noriko Miyake, Department of Human Genetics, Yokohama City University Graduate School of Medicine, 3-9, Fukuura, Kanazawa-ku, Yokohama 236-0004, Japan; nmiyake@yokohama-cu.ac.jp or Shiro Ikegawa, Laboratory of Bone and Joint Diseases, Center for Genomic Medicine, RIKEN 4-6-1 Shirokanedai, Minato-ku, Tokyo 108-8639, Japan; sikegawa@ims.u-tokyo.ac.jp

NM, NHE and AI contributed equally to this work.

Received 8 May 2012
Revised 8 June 2012
Accepted 10 June 2012

ABSTRACT

Background Brachyolmia is a heterogeneous group of skeletal dysplasias that primarily affects the spine. Clinical and genetic heterogeneity have been reported; at least three types of brachyolmia are known. *TRPV4* mutations have been identified in an autosomal dominant form of brachyolmia; however, disease genes for autosomal recessive (AR) forms remain totally unknown. We conducted a study on a Turkish family with an AR brachyolmia, with the aim of identifying a disease gene for AR brachyolmia.

Methods and results We examined three affected individuals of the family using exon capture followed by next generation sequencing and identified its disease gene, *PAPSS2* (phosphoadenosine-phosphosulfate synthetase 2). The patients had a homozygous loss of function mutation, c.337_338insG (p.A113GfsX18). We further examined three patients with similar brachyolmia phenotypes (two Japanese and a Korean) and also identified loss of function mutations in *PAPSS2*; one patient was homozygous for IVS3+2delT, and the other two were compound heterozygotes for c.616-634del19 (p.V206SfsX9) and c.1309-1310delAG (p.R437GfsX19), and c.480_481insCGTA (p.K161RfsX6) and c.661delA (p.I221SfsX40), respectively. The six patients had short-trunk short stature that became conspicuous during childhood with normal intelligence and facies. Their radiographic features included rectangular vertebral bodies with irregular endplates and narrow intervertebral discs, precocious calcification of rib cartilages, short femoral neck, and mildly shortened metacarpals. Spinal changes were very similar among the six patients; however, epiphyseal and metaphyseal changes of the tubular bones were variable.

Conclusions We identified *PAPSS2* as the disease gene for an AR brachyolmia. *PAPSS2* mutations have produced a skeletal dysplasia family, with a gradation of phenotypes ranging from brachyolmia to spondylo-epi-metaphyseal dysplasia.

INTRODUCTION

Brachyolmia is a heterogeneous group of skeletal dysplasias that primarily affects the spine. The name comes from the Greek for 'short trunk'; patients with brachyolmia have short stature due to a short trunk.[1] Conceptually, skeletal lesions of brachyolmia are limited to the spine; however, it is generally thought that pure brachyolmia (spine-only dysplasia) does not exist and that metaphyseal and/or epiphyseal involvements may be minimal and scattered, but are always present along with spinal involvements in cases labelled brachyolmia.[2]

Clinical and genetic heterogeneity have been reported in brachyolmia. At least three relatively well defined types of brachyolmia are known: type 1 that includes the Hobaek (OMIM 271530) and Toledo (OMIM 271630) forms; type 2 (OMIM 613678) referred to as the Maroteaux type; and type 3 (OMIM 113500). The former two types are autosomal recessive (AR) traits, while the latter is an autosomal dominant trait. Type 1 is characterised by scoliosis, platyspondyly with rectangular and elongated vertebral bodies, overfaced pedicles, and irregular and narrow intervertebral spaces. The Toledo form is distinguished from the Hobaek form by the presence of corneal opacity and precocious calcification of the costal cartilage.[3 4] Type 2 is distinguished by rounded vertebral bodies, less overfaced pedicles, minor facial anomalies, and precocious calcification of the falx cerebri.[1] Type 3 is characterised by severe kyphoscoliosis and flattened, irregular cervical vertebrae. Heterozygous mutations in the *TRPV4* (transient receptor potential vanilloid 4) gene (OMIM 605427) have been identified in several patients with type 3, autosomal dominant brachyolmia;[5 6] however, disease genes for recessive forms of brachyolmia remain totally unknown.

To identify novel disease genes from a limited number of subjects, exome sequencing (exon capture followed by next generation sequencing) is a promising approach. This approach sometimes presents us with unusual and unexpected connection between genes and phenotypes, thereby opening a new window for biology and medicine. We experienced a family with an AR form of brachyolmia harbouring three affected individuals. By performing exome sequencing for the family, we have identified the disease gene for the recessive brachyolmia, *PAPSS2* (phosphoadenosine-phosphosulfate synthetase 2). The discovery was confirmed by identification of *PAPSS2* mutations in three sporadic patients with different ethnic backgrounds but similar brachyolmia phenotypes. All patients had loss of function mutations of *PAPSS2* in both chromosomes.

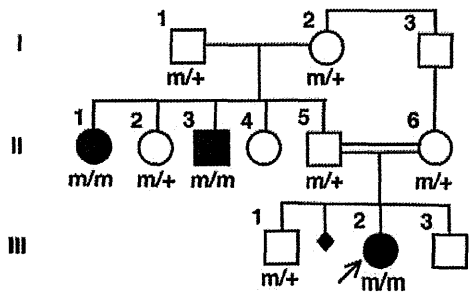

Figure 1 The pedigree of family 1 and co-segregation of the *PAPSS2* mutation (c.337_338insG) in the family. m: mutation allele, +: wild type allele.

MATERIALS AND METHODS

Subjects

P1-3 (family 1)

The proband (P1; III-2 in figure 1) was a Turkish girl referred to one of us (NHE) for genetic evaluation at the age of 8 years 4 months. She has been followed up for her spinal deformity and lumber pain elsewhere for 5 years. She was the result of a consanguineous (first cousin) marriage. A paternal uncle (P2; II-3 in figure 1) and aunt (P3; II-1 in figure 1) had the similar disease (table 1). The paternal grandparents originated from a small area and could be related. The inheritance of the disease was consistent with AR mode. Her birth length was 49 cm and weight 2800 g. She did not gain well after birth and was investigated for short stature at the age of 1 year. Her back deformity was noticed at around 3 years of age. On examination, she had short-trunk short stature. Her height was 109 cm (−3.2 SD), weight 29 kg (+0.38 SD) and head circumference 51 cm (−0.6 SD). She was mentally normal with no hearing or vision problems. She had widened wrists, bulbous proximal interphalangeal joints, clinodactyly of the fifth finger, and bowing deformity in her left lower leg. Serum DHEA-S (dehydroepiandrosterone-sulfate) was under the detection limit (<15.0 μg/dl).

Repeated skeletal surveys showed definite spondylodysplasia with minimal epiphyseal and metaphyseal changes, which was compatible with brachyolmia (table 1 and figure 2). Vertebral bodies were flat, particularly in thoracic spines. Endplates were irregular and intervertebral disc spaces were narrowed. The acetabular roof was horizontal. Femoral necks were slightly short. Metaphyses of the distal tibias had striation. Metacarpals were mildly shortened with mild metaphyseal changes. The bone age was advanced; 6 years 10 months at chronological age 5 years 8 months, and 10 years at chronological age 8 years 2 months (Greulich-Pyle method). MRIs and CTs showed no calcification of the falx cerebri.

At her last visit (10 years 4 months old), she had increasing back deformity and pain. Her height was 121 cm (−3.4 SD), arm span 119 cm, and sitting/standing height ratio was 0.53.

Table 1 Clinical and radiographic phenotypes of autosomal recessive brachyolmina harbouring *PAPSS2* mutation (in comparison to those in spondylo-epi-metaphyseal dysplasia Pakistani type)

Patient ID	P1	P2	P3	P4	P5	P6	
Family	Family 1						Patient reported by Noordam *et al*
Intra-family ID	III-2	II-3	II-1	Family 2	Family 3	Family 4	
Country of origin	Turkey			Japan	Japan	Korea	Turkey
Sex	Female	Male	Female	Female	Female	Male	Female
Age at first presentation	8 years 4 months	29 years	40 years	11 years 4 months	8 years 8 months	12 years 7 months	8 years
Birth length (cm)	49	NA	NA	46	47	50	NA
Birth weight (g)	2800	NA	NA	3340	2676	3100	NA
Consanguinity of the parents	+	Probably +	Probably +	(−)	(−)	(−)	(−)
Clinical feature							
Normal intelligence	+	+	+	+	+	+	NA
Normal facies	+	+	+	+	+	+	NA
Short-trunk short stature	+	+	+	+	+	+	+
Spinal deformity	Kyphosis	(−)	Kyphosis, lumbar scoliosis	Kyphosis	(−)	(−)	Lumbar scoliosis
Leg deformity	Bil genu varum and internal rotation	(−)	Bil genu varum and internal rotation	(−)	Right genu valgum	Bil genu varum	NA
Androgen excess sign	(−)	(−)	(−)	(−)	(−)	(−)	+
Radiographic feature							
Rectangular vertebra	+	+	+	+	+	+	+
Irregular endplate	+	+	+	+	+	+	+
Narrowed disc	+	+	+	+	+	+	+
Precocious calcification of costal cartilage	(−)	+	+	+	(−)	(−)	NA
Delayed ossification of hip and knee epiphyses	(−)	NA	NA	(−)	(−)	(−)	(−)
Early osteoarthritic change	(−)*	(−)	(−)	(−)	(−)*	(−)*	(−)*
Short femoral neck	+	+	+	+	+	+	+
Metaphyseal abnormality†	Dist tibia	Prox tibia	Prox tibia	(−)	(−)	Prox tibia	(−)
Mild brachymetacarpia	+	+	+	+	+	+	+
Advanced bone age	+	NA	NA	+	+	+	+

*May be too young to be evaluated.
†Other than short femoral neck and fingers.
Bil, bilateral; Dist, distal; NA, not available or assessed; Prox, proximal.

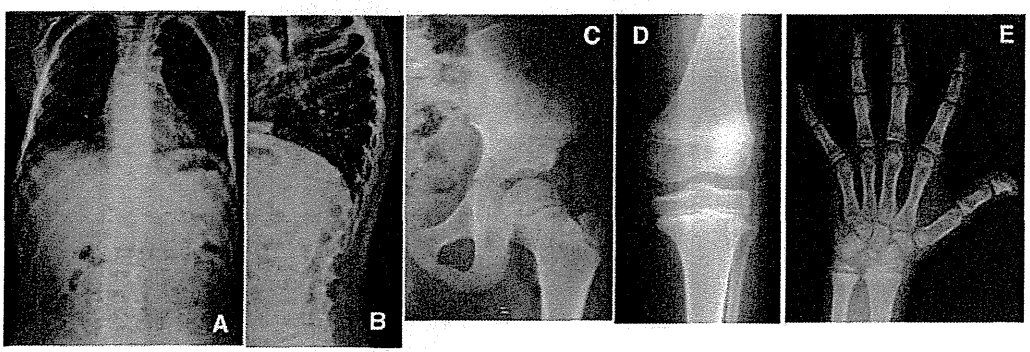

Figure 2 Radiographs of P1 (III-2 in family 1) at age 8.5 years. (A) Spine anteroposterior (AP). Mildly overfaced vertebra. (B) Lateral spine. Mild flattening of vertebral bodies and irregular endplates. (C) Left hip AP. Almost normal epiphysis. (D) Left knee AP. Epiphyseal and metaphyseal abnormalities are unremarkable. (E) Left hand AP. Metacarpals are mildly shortened with mild irregularity of the growth plates. Epiphyses of the distal radius and ulna show mild dysplasia. The bone age is advanced.

Breast development was Tanner 2–3, pubic hair Tanner 1. There had been no sign of androgen excess (acne, hirsutism, etc).

P4-6 (sporadic cases)

After we found *PAPSS2* mutations in family 1, we reviewed the patient registry of the Japanese Skeletal Dysplasia Consortium and found two Japanese patients (P4-5) and one Korean patient (P6) who had similar phenotypes to those of the Turkish family (table 1 and figure 3); all three were sporadic cases from normal, non-consanguineous parents and were *TRPV4* mutation negative.

DNA sample

Genomic DNA was extracted by standard procedures from peripheral blood of the patients and/or their family members after informed consent. The study was approved by the ethical committee of RIKEN, Yokohama City University, and participating institutions.

Exome sequencing

Three affected individuals of family 1 (II-1, II-3 and III-2) were analysed by whole exome sequencing as previously reported (see supplementary online table S1).[7 8] In brief, 3 μg of genomic DNA was sheared by Covaris S2 system (Covaris, Woburn, Massachusetts, USA) and processed using a SureSelect Human All Exon 50 Mb Kit (Agilent Technologies, Santa Clara, California, USA) according to the manufacturer's instructions. DNAs were captured by the kit and were sequenced by GAIIx (Illumina, San Diego, California, USA) with 108 pair-ends reads. Each sample was run in one lane. Image analysis and base calling were performed by sequence control software 2.9 and real time analysis 1.9 (Illumina), and CASAVA software V.1.8.1 (Illumina). The quality-controlled (path-filtered) reads were mapped to human genome reference hg19 with Mapping and Assembly with Qualities (MAQ, http://maq.sourceforge.net/) and NextGENe software V.2.00 (SoftGenetics, State College, Pennsylvania, USA). The variants from MAQ were annotated by SeattleSeq annotation 131 (http://snp.gs.washington.edu/SeattleSeqAnnotation131/).

Priority scheme

Variants were filtered by the following conditions using the script created by BITS (Tokyo, Japan): (1) variants only annotated on human autosomes and chromosome X; (2) variants not in dbSNP131, dbSNP134, the 1000 Genomes database (http://www.1000genomes.org/), and in-house exome data of normal Japanese controls (n=66); (3) variants that were non-synonymous and intronic changes (±20 bp from exon/intron boundaries) called in common by NextGENe and MAQ, and variants of insertion/deletion with a NextGENe score ≥10. The variant numbers in each category are shown in supplementary online table S1.

Sanger sequencing and evaluation of mutations

To confirm the sequence change identified in P1-3 by the exome sequencing, exon 3 of *PAPSS2* and its flanking intronic sequences (The GenBank reference sequence: NM_001015880) were amplified by PCR from genomic DNA. To examine *PAPSS2* mutation in P4-6, all exons of *PAPSS2* and its flanking intronic sequences were amplified by PCR from genomic DNA. Primer sequences and PCR conditions were as previously described.[9] PCR products were directly sequenced using ABI Prism automated sequencers 3730 (PE Biosystems, Foster City, CA, USA).

To evaluate the possibility of polymorphisms, identified sequence changes were genotyped in 93 ethnically matched controls using the invader assay coupled with PCR as described previously.[10] The sequence changes were evaluated by public databases including OMIM (http://www.ncbi.nlm.nih.gov/omim) and dbSNP (http://www.ncbi.nlm.nih.gov/projects/SNP/).

RESULTS

Exome sequencing

A total of 90 964 194 (II-1), 90 508 738 (II-3) and 90 223 680 (III-2) reads were mapped to the whole human genome in pairs by MAQ. Considering the consanguinity of the family, we focused on the same homozygous mutations shared by the three affected individuals. After filtering, a total of 37 homozygous variants remained as candidates (23 missense, 11 intronic, and three insertion changes) (see supplementary online table S1). Among them, one base pair insertion, c.337_338insG in exon 3 of *PAPSS2*, was highlighted because it is a causative gene for SEMD, Pakistani type (OMIM 612847), that has overlapping features with the phenotypes of the three patients.

The insertion sequence was confirmed by direct sequence of PCR products from genomic DNA. Direct sequencing of nine family members showed co-segregation of the mutation with the disease phenotype (figure 1). The insertion mutation was

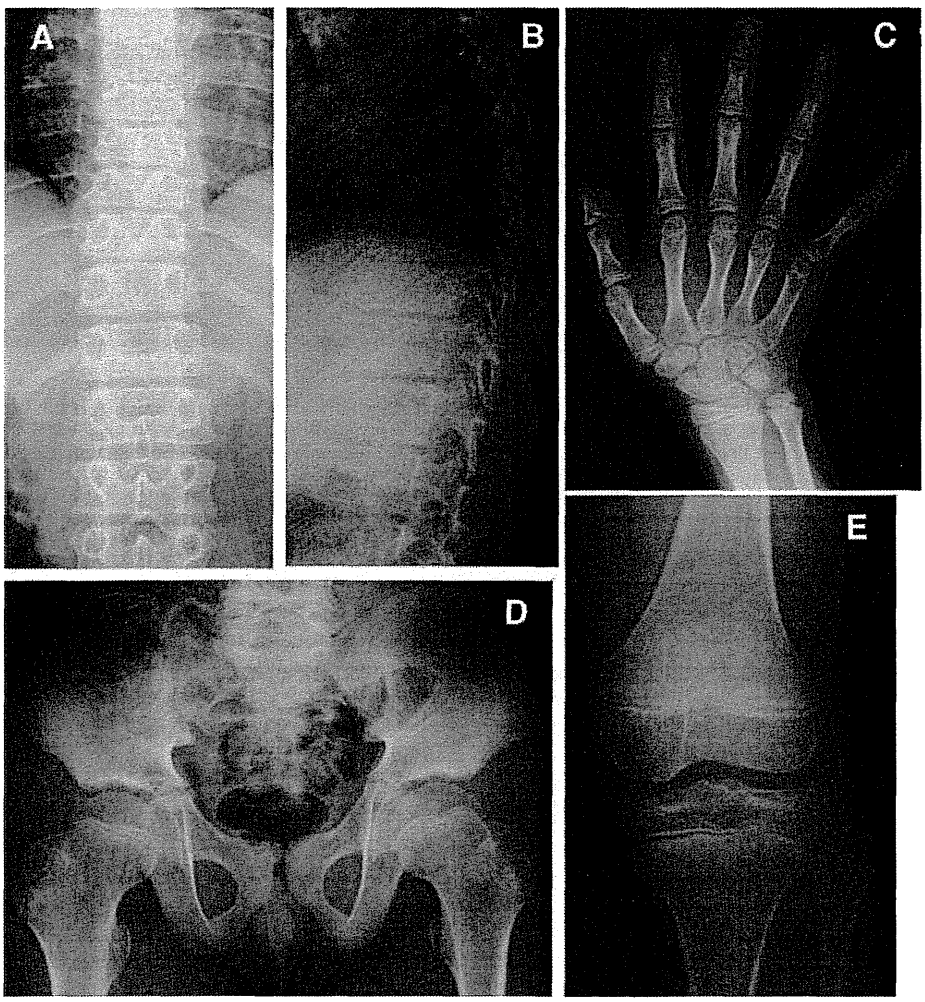

Figure 3 Radiographs of P5 at age 8 years 8 months. (A) Spine anteroposterior (AP). Platyspondyly. Over-faced pedicle is not so distinct. (B) Spine lateral. Flattened vertebral bodies and narrow disc spaces. (C) The right hand AP. Slightly short metacarpals. Phalanges are not so short. The bone age is advanced (12 years by the Greulich-Pyle method). (D) Pelvis AP. Short femoral neck and horizontal acetabulum. Proximal epiphyses are normal. (E) The right knee AP. Unremarkable changes. No fibula overgrowth.

predicted to create a premature stop codon (p.A113GfsX18), thereby most probably resulting in a null allele due to nonsense mutation mediated RNA decay (NMD).[11] The mutation was not found in the public mutation database and sequence variation database. Also, it was not found in 93 ethnically matched controls examined by Invader assay.[10]

Identification of *PAPSS2* mutations in sporadic cases

We screened for *PAPSS2* mutations in P4-6 by direct sequencing as previously described.[9] We found *PAPSS2* mutations in both chromosomes of all subjects (table 2). All mutations are predicted to create premature stop codons before the second last exon of the gene. Therefore, they are most likely to result in null alleles due to NMD. P5 was a homozygote, and P4 and P6 were heterozygotes for the mutations. Compound heterozygosity of the subjects was confirmed by sequencing of the parents' genomic DNA. All these mutations were not found in 93 ethnically matched controls examined by Invader assay[10] nor in public databases.

Phenotypes of the patients with *PAPSS2* mutations

Clinical features of our six patients were short-trunk short stature with short neck (table 1). The short stature was noticeable early in life, but not always at birth; it usually became definite after age 5–6 years. All patients had normal intelligence and facies. Corneal opacity was not found. Kyphosis and/or scoliosis were found in three subjects. Bone age was advanced in all (4/4) cases evaluated. No clinical sign of androgen excess was noted in all (6/6) patients and their family members. The main radiographic feature was pronounced flattening of spine (rectangular vertebral body), particularly in the thoracic spine, which accompanied irregular

Table 2 *PAPSS2* mutations in autosomal recessive brachyolmia

Family	Exon	Nucleotide change	Amino acid change
1	3	c.337_338insG (homozygous)	p.A113GfsX18
2	5	c.616-634del19	p.V206SfsX9
	11	c.1309-1310delAG	p.R437GfsX19
3	3	IVS3+2delT (homozygous)	p.L50SfsX2
4	4	c.480_481insCGTA	p.K161RfsX6
	6	c.661delA	p.I221SfsX40

The nucleotide changes are shown with respect to *PAPSS2* mRNA sequence (NM_001015880). The corresponding predicted amino acid changes are numbered from the initiating methionine residue. Exons are numbered sequentially 1–13.

endplates and narrow disc spaces. Mild shortening of the femoral neck and metacarpals were common features. The costal cartilages showed precocious calcification in the adult subjects (3/3). Epiphyseal and metaphyseal dysplasias were very mild, if present. From these features of spine predominant dysplasia, our patients can be diagnosed as having brachyolmia. Among known types of brachyolmias, characteristics of the Hobaek and Toledo types are mixed.[1 4]

DISCUSSION

PAPSS2 mutation has been reported to be responsible for two other overlapping, but distinct, phenotypes. The first is SEMD Pakistani type; Ahmad *et al*[12] described a large consanguineous Pakistani family with a distinct form of SEMD with autosomal inheritance. Its clinical features include short stature evident at birth, short and bowed lower limbs, mild brachydactyly, kyphoscoliosis, enlarged knee joints, and precocious osteoarthropathy. Radiographic features are platyspondyly with irregular endplates and narrowed joint spaces, delayed epiphyseal ossification at the hips and knees, diffuse early osteoarthritic changes primarily in the spine and hands, and mild brachydactyly. Metaphyseal abnormalities are seen predominantly in the hips and knees. This disease is differentiated from other forms of SEMD by its mild degree of metaphyseal involvement, type of brachydactyly, and the absence of loose joints or other clinical findings. A homozygous nonsense mutation of *PAPSS2* (S438X) is identified in all affected individuals in the family.[13] Many of the characteristics of SEMD Pakistani type, including enlarged joints with deformity, delayed epiphyseal ossification at the hips and knees, and precocious osteoarthritic changes of the large and small joints, are absent in our cases (table 1).

PAPSS2 mutations have also been found in a patient with a different phenotype, spondylodysplasia and premature pubarche.[9] A Turkish girl with premature pubarche, hyperandrogenic anovulation, short stature, and skeletal dysplasia showed a compound heterozygosity for a missense and a nonsense mutation in *PAPSS2*: the former was a 143C>G transversion resulting in a T48R substitution at a conserved residue in the adenosine 5-prime-phosphosulfate kinase domain, and the latter was a 985C>T transition resulting in R329X. Their functional assays revealed no detectable activity for R329X, and only minor residual activity for T48R (6% of the wild type activity). The mother who carried the R329X mutation had normal pubarche and menarche, but developed obesity, oligomenorrhoea, and hirsutism in her fourth decade, while the father who carried the T48R mutation showed normal growth and pubertal development. The skeletal changes in this patient are more similar to those of our cases than SEMD Pakistani type (table 1).

Among our patients, spinal changes were very similar, but epiphyseal and metaphyseal changes were considerably variable (table 1). P4 and P5, similar to the case reported by Noordam *et al*,[9] showed minimal epiphyseal and metaphyseal dysplasias. P6 had considerable epi-metaphyseal changes in the long bones of the lower extremities; they were more severe than those in family 1 (P1-3), but were far milder than those in SEMD Pakistani type. The differential diagnosis includes AR spondyloepiphyseal dysplasia tarda[14] because of late manifestation, AR inheritance, and relatively mild spondyloepiphyseal dysplasia with flat vertebral bodies with irregular endplates. In the disorder, overfaced vertebral bodies is absent and the capital femoral epiphyses are severely affected.[14]

In a form of autosomal dominant brachyolmia, heterozygous *TRPV4* mutation has been identified.[5 6] Notably, the *TRPV4* mutation presents a wide phenotypic gradation from brachyolmia at its most mild, through spondylometaphyseal dysplasia type Kozlowski, spondyloepiphyseal dysplasia type Maroteaux, and metatropic dysplasia, to parastremmatic dysplasia and fetal akinesia at its most severe.[5 15–17] *PAPSS2* mutations might also present a phenotype gradation from brachyolmia to spondylo-epiphyseal and spondylo-epimetaphyseal dysplasia like SEMD Pakistani type. Further investigation of *PAPSS2* mutations in brachyolmia and skeletal dysplasias with overlapping phenotypes to our cases as well as other cases with *PAPSS2* mutations[9 14] would provide further answers.

An additional supplementary table is published online only. To view this file please visit the journal online (http://jmg.bmj.com)

Acknowledgements We thank the patients and their family for their help to the study. We also thank the Japanese Skeletal Dysplasia Consortium.

Contributors NM performed the exome experiments, analysed the data, wrote the paper, and is guarantor. NE and PI collected family samples and evaluated their phenotypes. AI performed the sequence experiments, analysed the data, and wrote the paper. JD performed the experiments. NoM, KM, TC, OK, and TN collected samples and evaluated their clinical and radiographic phenotypes. TH and GN analysed the clinical data. HO collected and controlled the experimental samples. NaM performed the experiments and analysed the data. SI analysed the data, wrote the paper, and is also guarantor. All authors have critically revised the paper.

Funding This study is supported by research grants from the Ministry of Health, Labour and Welfare (23300101: S Ikegawa and N Matsumoto; 23300102: T Hasegawa; 23300201: S Ikegawa), by a Grant-in-Aid for Young Scientists from the Japan Society for the Promotion of Science (N Miyake), and by Research on intractable diseases, Health and Labour Sciences Research Grants, H23-Nanchi-Ippan-123 (S Ikegawa).

Patient consent Obtained.

Ethics approval This study was performed under the approval of the ethical committee of RIKEN, Yokohama City University, and participating institutions.

Provenance and peer review Not commissioned; externally peer reviewed.

Data sharing statement Additional unpublished data on mutation examination are available on request to researchers.

REFERENCES

1. **Shohat M,** Lachman R, Gruber HE, Rimoi DL. Brachyolmia: radiographic and genetic evidence of heterogeneity. *Am J Med Genet* 1989;**33**:209–19.
2. **Kozlowski K,** Beemer FA, Bens G, Dijkstra PF, Iannaccone G, Emons D, Lopez-Ruiz P, Masel J, van Nieuwenhuizen O, Rodriguez-Barrionuevo C. Spondylo-Metaphyseal Dysplasia (Report of 7 cases and essay of classification). *Prog Clin Biol Res* 1982;**104**:89–101.
3. **McKusick VA.** Medical genetics. A 40-year perspective on the evolution of a medical specialty from a basic science. *JAMA* 1993;**270**:2351–6.
4. **Hoo JJ,** Oliphant M. Two sibs with brachyolmia type Hobaek: five year follow-up through puberty. *Am J Med Genet A* 2003;**116A**:80–4.
5. **Rock MJ,** Prenen J, Funari VA, Funari TL, Merriman B, Nelson SF, Lachman RS, Wilcox WR, Reyno S, Quadrelli R, Vaglio A, Owsianik G, Janssens A, Voets T, Ikegawa S, Nagai T, Rimoin DL, Nilius B, Cohn DH. Gain-of-function mutations in TRPV4 cause autosomal dominant brachyolmia. *Nat Genet* 2008;**40**:999–1003.
6. **Dai J,** Cho TJ, Unger S, Lausch E, Nishimura G, Kim OH, Superti-Furga A, Ikegawa S. TRPV4-pathy, a novel channelopathy affecting diverse systems. *J Hum Genet* 2010;**55**:400–2.
7. **Doi H,** Yoshida K, Yasuda T, Fukuda M, Fukuda Y, Morita H, Ikeda S, Kato R, Tsurusaki Y, Miyake N, Saitsu H, Sakai H, Miyatake S, Shiina M, Nukina N, Koyano S, Tsuji S, Kuroiwa Y, Matsumoto N. Exome sequencing reveals a homozygous SYT14 mutation in adult-onset, autosomal-recessive spinocerebellar ataxia with psychomotor retardation. *Am J Hum Genet* 2011;**89**:320–7.
8. **Tsurusaki Y,** Okamoto N, Ohashi H, Kosho T, Imai Y, Hibi-Ko Y, Kaname T, Naritomi K, Kawame H, Wakui K, Fukushima Y, Homma T, Kato M, Hiraki Y, Yamagata T, Yano S, Mizuno S, Sakazume S, Ishii T, Nagai T, Shiina M, Ogata K, Ohta T, Niikawa N, Miyatake S, Okada I, Mizuguchi T, Doi H, Saitsu H, Miyake N, Matsumoto N. Mutations affecting components of the SWI/SNF complex cause Coffin-Siris syndrome. *Nat Genet* 2012;**44**:376–8.
9. **Noordam C,** Dhir V, McNelis JC, Schlereth F, Hanley NA, Krone N, Smeitink JA, Smeets R, Sweep FC, Claahsen-van der Grinten HL, Arlt W. Inactivating PAPSS2 mutations in a patient with premature pubarche. *N Engl J Med* 2009;**360**:2310–18.

10. **Ohnishi Y,** Tanaka T, Ozaki K, Yamada R, Suzuki H, Nakamura Y. A high-throughput SNP typing system for genome-wide association studies. *J Hum Genet* 2001;**46**:471–7.
11. **Holbrook JA,** Neu-Yilik G, Hentze MW, Kulozik AE. Nonsense-mediated decay approaches the clinic. *Nat. Genet* 2004;**36**:801–8.
12. **Ahmad M,** Haque MF, Ahmad W, Abbas H, Haque S, Krakow D, Rimoin DL, Lachman RS, Cohn DH. Distinct, autosomal recessive form of spondyloepimetaphyseal dysplasia segregating in an inbred Pakistani kindred. *Am J Med Genet* 1998;**78**:468–73.
13. **Faiyaz ul Haque M,** King LM, Krakow D, Cantor RM, Rusiniak ME, Swank RT, Superti-Furga A, Haque S, Abbas H, Ahmad W, Ahmad M, Cohn DH. Mutations in orthologous genes in human spondyloepimetaphyseal dysplasia and the brachymorphic mouse. *Nat Genet* 1998;**20**:157–62.
14. **Leroy JG,** Leroy BP, Emmery LV, Messiaen L, Spranger JW. A new type of autosomal recessive spondyloepiphyseal dysplasia tarda. *Am J Med Genet A* 2004;**125A**:49–56.
15. **Krakow D,** Vriens J, Camacho N, Luong P, Deixler H, Funari TL, Bacino CA, Irons MB, Holm IA, Sadler L, Okenfuss EB, Janssens A, Voets T, Rimoin DL, Lachman RS, Nilius B, Cohn DH. Mutations in the gene encoding the calcium-permeable ion channel TRPV4 produce spondylometaphyseal dysplasia, Kozlowski type and metatropic dysplasia. *Am J Hum Genet* 2009;**84**:307–15.
16. **Nishimura G,** Dai J, Lausch E, Unger S, Megarbané A, Kitoh H, Kim OH, Cho TJ, Bedeschi F, Benedicenti F, Mendoza-Londono R, Silengo M, Schmidt-Rimpler M, Spranger J, Zabel B, Ikegawa S, Superti-Furga A. Spondylo-epiphyseal dysplasia, Maroteaux type (pseudo-Morquio syndrome type 2), and parastremmatic dysplasia are caused by TRPV4 mutations. *Am J Med Genet A* 2010;**152A**:1443–9.
17. **Unger S,** Lausch E, Stanzial F, Gillessen-Kaesbach G, Stefanova I, Di Stefano CM, Bertini E, Dionisi-Vici C, Nilius B, Zabel B, Superti-Furga A. Fetal akinesia in metatropic dysplasia: The combined phenotype of chondrodysplasia and neuropathy? *Am J Med Genet A* 2011;**155A**:2860–4.

Journal of Human Genetics (2012) 57, 804–806

www.nature.com/jhg

SHORT COMMUNICATION

Sibling cases of moyamoya disease having homozygous and heterozygous c.14576G>A variant in *RNF213* showed varying clinical course and severity

Satoko Miyatake[1], Hajime Touho[2], Noriko Miyake[1], Chihiro Ohba[1], Hiroshi Doi[1], Hirotomo Saitsu[1], Masataka Taguri[3], Satoshi Morita[3] and Naomichi Matsumoto[1]

Moyamoya disease (MMD) is a rare cerebrovascular disease characterized by progressive occlusion of the terminal portion of the internal carotid arteries and their branches. A genetic background was under speculation, because of the high incidence of familial occurrence. Sibling cases usually exhibit a similar clinical course. Recently, *RNF213* was identified as the first MMD susceptibility gene. The c.14576G>A variant of *RNF213* significantly increases the MMD risk, with an odds ratio of 190.8. Furthermore, there is a strong association between clinical phenotype and the dosage of this variant. The present study described sibling MMD cases having homozygous and heterozygous c.14576G>A variant in *RNF213*, as well as different clinical course and disease severity. The homozygote of c.14576G>A variant showed an early onset age and rapid disease progress, which resulted in significant neurological deficits with severe and wide distribution of vasculopathy. In contrast, the heterozygote of the variant showed a relatively late-onset age and mild clinical course without irreversible brain lesions with limited distribution of vasculopathy. This is the first report of sibling MMD cases with different doses of the *RNF213* variant, showing its genetic impact on clinical phenotype even in members with similar genetic background.
Journal of Human Genetics (2012) **57**, 804–806; doi:10.1038/jhg.2012.105; published online 30 August 2012

Keywords: cerebrovascular disease; gene dose effect; moyamoya disease; *RNF213*; sibling cases

Moyamoya disease (MMD) is a rare cerebrovascular disease characterized by progressive occlusion of terminal portions of the internal carotid arteries (ICAs) and their distal branches, which is later accompanied by compensatory recruitment of an abnormal vascular network termed the 'moyamoya' vessels.[1] MMD is a relatively common cause of pediatric stroke,[2,3] which might lead to irreversible and devastating neurological deficits and intellectual impairments if left untreated. Genetic factors have been speculated, because of the high incidence of familial occurrence. Recently, the first MMD susceptibility gene, *RNF213*, was reported.[4,5] The c.14576G>A variant of *RNF213* is a missense variant that switches arginine to lysine; the variant has been shown to significantly increase the risk of MMD with an odds ratio of 190.8.[4] In addition, c.14576G>A homozygotes exhibit more severe and wider vasculopathy than heterozygotes.[6] Here, we present sibling cases of MMD having homozygous and heterozygous c.14576G>A variant in *RNF213*, as well as different clinical course and disease severity.

The cases are Japanese siblings born to nonconsanguineous, healthy unaffected parents. They had a brother without MMD (Figure 1a). Case 1 (proband) is a 21-year-old male. His pregnancy and delivery were unremarkable and he exhibited normal psychomotor development. He had a first history of transient ischemic attack (TIA) associated with left-sided weakness at age 2, and was subsequently diagnosed with MMD. Bilateral encephalo-duro-arterio-synangiosis (EDAS)[7] was performed 2 months after the initial TIA. However, left hemiparesis persisted after surgery. Brain computed tomography (CT) results revealed a low-density area in the territory of right middle cerebral artery (MCA), and the right cerebral hemisphere was atrophic. An older ischemic lesion was also present in the right occipital region. Cerebral angiograms demonstrated that right ICA, MCA and anterior cerebral artery (ACA) were steno-occlusive with a poor moyamoya vascular network. Left ICA, MCA and ACA were also stenotic, but an abundant moyamoya vascular network was observed. Bilateral frontal omental transplantation[8] was performed at age 3. At 5 years of age, TIAs associated with visual disturbance frequently occurred, and bilateral occipital gracilis muscle transplantation[9] was performed. Following surgery, the TIAs disappeared. Intellectual ability was slowly deteriorating. At age 9, his total intelligence quotient (IQ) was 68, verbal IQ was 73 and performance IQ was 68. At age 12, he suffered repetitive TIAs associated with right-sided

[1]Department of Human Genetics, Yokohama City University Graduate School of Medicine, Yokohama, Japan; [2]Department of Neurosurgery, Touho Neurosurgical Clinic, Osaka, Japan and [3]Department of Biostatistics and Epidemiology, Yokohama City University Medical Center, Yokohama, Japan
Correspondence: Dr S Miyatake, Department of Human Genetics, Yokohama City University Graduate School of Medicine, 3-9 Fukuura, Kanazawa-ku, Yokohama 236-0004, Japan.
E-mail: miyatake@yokohama-cu.ac.jp
Received 26 March 2012; revised 27 July 2012; accepted 6 August 2012; published online 30 August 2012

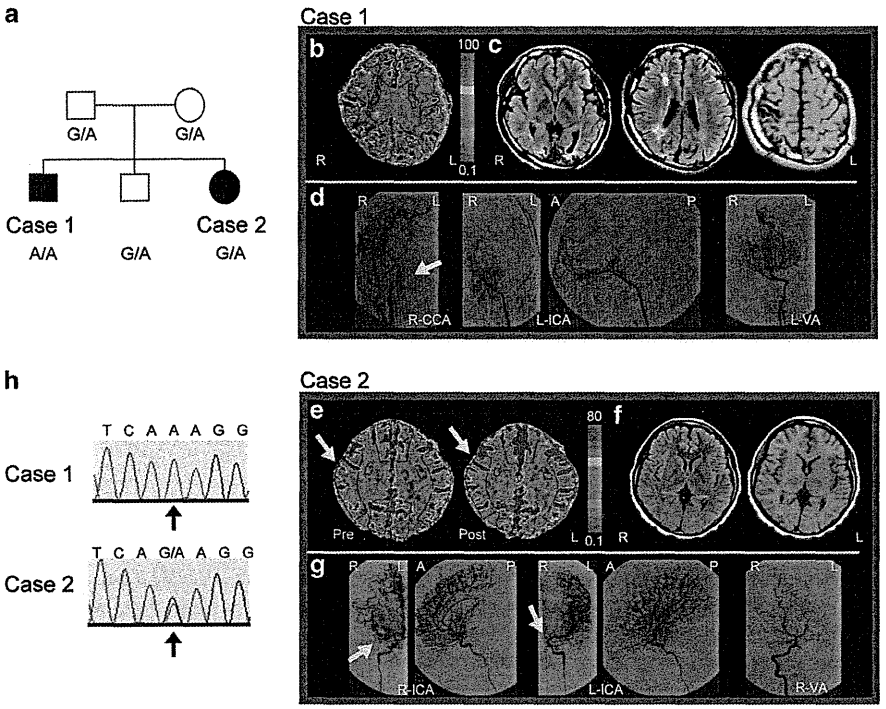

Figure 1 (**a**) Family pedigree showing the genotype of c.14576G>A variant. G/A: heterozygous c.14576G>A variant; A/A: homozygous c.14576G>A variant. (**b**) Stable xenon-enhanced CT of case 1 at age 12 shows decreased cerebral blood flow, especially in the left cerebral hemisphere. (**c**) Brain MRI (fluid-attenuated inversion recovery image (left and middle images) of case 1 at age 21, showing high-intensity lesions in bilateral occipital, right MCA territory including the watershed region, and the left semiovale. The right temporo-parietal lesion accompanies brain atrophy in the T1-weighted image (right image). (**d**) Cerebral angiograms of case 1 at age 21. Bilateral ICAs and PCAs are occluded. From right to left: R-CCA: A-P view; L-ICA: A-P view and lateral view; L-VA: A-P view. (**e**) Stable xenon-enhanced CT of case 2 at age 17 shows decreased cerebral vasoreactivity in the right frontotemporal area, comparing pre- and post-intravenous acetazolamide administration. CVR was 9.4% for the right and 23.3% for the left frontotemporal area, respectively. (**f**) Fluid-attenuated inversion recovery (left) and T1-weighted (right) images of brain MRI in case 2 at age 17 showing no abnormalities. (**g**) Cerebral angiograms of case 2 at age 17 reveal a stenotic right proximal portion of the MCA (M1), and retrograde filling from the right ACA to the MCA territory was observed. The left proximal portion of the ACA (A1) was also stenotic, and partial retrofilling from the left MCA to the left ACA territory *via* leptomeningeal anastomosis was observed. From right to left: R-ICA: A-P view and lateral view; L-ICA: A-P view and lateral view; R-VA: A-P view. (**h**) Electropherogram of the c.14576G>A variant (arrow) in *RNF213*. Case 1 expresses the homozygous c.14576G>A variant, and case 2 expresses the heterozygous variant. A, anterior; CCA, common carotid artery; L, left; P, posterior; R, right; VA, vertebral artery.

weakness. A cerebral blood flow study with stable xenon-enhanced CT showed a diffuse decrease, especially in the left cerebral hemisphere (Figure 1b). A subcutaneous tissue graft, which included a parietal branch of the left superficial temporal artery and a relevant vein,[10] was transplanted in the left parietal lobe, and TIAs subsequently decreased. At present, mild to moderate hemiparesis was observed on both sides. He can perform basic activities of daily living independently, including self-feeding using chopsticks. TIAs associated with bilateral weakness of lower extremities and dysarthria occur less than once a month. Frequent fore-headache remained. Brain magnetic resonance imaging (MRI) obtained at age 21 showed multiple infarctions with brain atrophy, with no gross interval changes since the previous surgery (Figure 1c), and cerebral angiograms demonstrated bilateral ICA and posterior cerebral artery (PCA) occlusion (Figure 1d).

Case 2 was an 18-year-old female, who was the younger sister of the proband. Her pregnancy and delivery were unremarkable, and she exhibited normal psychomotor development. Her initial attack occurred as TIA associated with weakness and numbness of the left hand at age 17. On her admission to the neurosurgical clinic, no abnormal neurological findings were observed. Cerebral vasoreactivity to intravenous acetazolamide administration, evaluated by stable xenon-enhanced CT,[11] was decreased in the right hemisphere (Figure 1e), although brain MRI showed normal findings (Figure 1f). Cerebral angiograms revealed that the right proximal portion of the MCA (M1) and left proximal portion of the ACA (A1) were stenotic (Figure 1g). Case 2 was diagnosed with MMD, and right superficial temporal artery–MCA anastomosis[12] was performed 2 months after diagnosis. Then, the TIAs completely disappeared.

Both parents were examined by brain MRI/MR angiography (MRA) during their 20s or 30s, and the unaffected sibling, who was 20 years old at the time of the study, underwent a brain MRI/MRA at the age of 2. Results were normal for all of them.

Following written informed consent, genomic DNA from the affected siblings and unaffected family members was obtained from either peripheral blood leukocytes or saliva. The mutation analysis of *RNF213* (GenBank accession number, NM_020914.4) was performed by high-resolution melting analysis and direct sequencing. The homozygous c.14576G>A variant in *RNF213* was identified in case 1, and the heterozygous variant was identified in case 2 and all other unaffected family members (father, mother and unaffected sibling). No other mutation was identified in the entire *RNF213* gene (Figure 1h).

Table 1 Case profiles

Clinical features	*Case 1*	*Case 2*
Age at onset (yo)	2	17
Transient ischemic attack	+	+
Cerebral infarction	+	–
Intracerebral/intraventricular hemorrhage	–	–
Headache	+	–
Paresis	+	–
Seizure	–	–
Visual defects	+	–
Intellectual impairment	+	–
Present modified Rankin scale	2	0
Brain MRI findings	Multiple infarctions with brain atrophy	Normal study
Distribution of vasculopathy		
ICA	Bilateral occlusion	–
ACA	Bilateral occlusion	lt stenosis
MCA	Bilateral occlusion	rt stenosis
PCA	Bilateral occlusion	–
Other	–	–
Surgical history	2-yo bilateral EDAS 3-yo bilateral frontal omental plantation 5-yo bilateral gracilis muscle plantation 12-yo lt. STA-STV graft on left parietal lobe	17-yo rt. STA-MCA anastomosis
RNF213 genotype	Homozygous c.14576G>A	Heterozygous c.14576G>A

Abbreviations: ACA, anterior cerebral artery; EDAS, encephalo-duro-arterio-synangiosis; ICA, internal carotid artery; lt, left; MCA, middle cerebral artery; PCA, posterior cerebral artery; rt, right; STA, superficial temporal artery; STV, superficial temporal vein; yo, years old.

Several reports on sibling MMD cases have revealed a tendency towards similar onset age and similar clinical courses.[13,14] These similarities could be due to similar genetic and environmental backgrounds that the siblings share. The present cases, however, were rather atypical. Case 1, a homozygote of c.14576G>A variant, exhibited an early-onset age and rapid disease progress, which resulted in significant neurological deficits. Cerebral angiograms revealed severe and wide distribution of vasculopathy. In contrast, case 2, the heterozygote of the variant, exhibited a relatively late-onset age and mild clinical course without irreversible brain lesions. Vasculopathy of case 2 appeared milder and exhibited more limited distribution than case 1 (Table 1). The differences in clinical phenotypes between the siblings could be explained by different genetic backgrounds: one had two copies of the c.14576G>A variant and the other had only one copy. Present cases give us another evidence that clinical phenotypes of MMD are associated with a dose effect of the heterozygous and homozygous c.14576G>A variants of *RNF213*. This variant might have a much larger impact on MMD phenotype than common variants of other common diseases.

Why there are both heterozygote of this variant with and without MMD is a difficult question, as it is unclear how much risk one would own with this variant. To solve this, we calculated the life-time incidence rate of MMD if one Japanese has the heterozygous c.14576G>A variant. It was reported that heterozygotes were identified in 153/204 (75%) of patients with MMD, and in 5/283 (1.8%) of normal Japanese controls.[6] Annual incidence is estimated at 0.35–0.94 per 100 000 person-years in Japan.[15,16] Appling the Bayes' theorem with these data, the life-time incidence rate of MMD having heterozygous was calculated to be 1.44–3.77%. It is suggested that the incidence rate of MMD is relatively low if one had the heterozygous variant, whereas incidence rate for homozygotes are extremely high (>78%).[6] This also reflects the effect of this variant with the dose effect.

In conclusion, a family with sibling MMD cases having different doses of the *RNF213* variant is first described, clearly showing impact of the variant on clinical phenotype even in members with similar genetic background.

ACKNOWLEDGEMENTS

We thank all the participants for their cooperation in this study. We also thank Ms Y Yamashita, Dr K Nishiyama, Ms K Takabe, Mr T Miyama and Ms E Koike from the Department of Human Genetics, Yokohama City University, Graduate School of Medicine, for their technical assistance. This study was supported by a grant from the Ministry of Health, Labor and Welfare, the Japan Science and Technology Agency (NM, HS and NMiyake), a Grant-in-Aid for Scientific Research on Innovative Areas (Foundation of Synapse and Neurocircuit Pathology) from the Ministry of Education, Culture, Sports, Science, and Technology of Japan (NM), a Grant-in-Aid for Scientific Research from the Japan Society for the Promotion of Science (NM), a grant from the Takeda Science Foundation(NM), and a Grant-in-Aid for Young Scientists from the Japan Society for the Promotion of Science (HS and NMiyake), a Grant-in-Aid for Japan Foundation for Neuroscience and Mental Health (SM).

1 Suzuki, J. & Takaku, A. Cerebrovascular 'moyamoya' disease. Disease showing abnormal net-like vessels in base of brain. *Arch. Neurol.* **20,** 288–299 (1969).
2 Bigi, S., Fischer, U., Wehrli, E., Mattle, H. P., Boltshauser, E., Burki, S. *et al.* Acute ischemic stroke in children versus young adults. *Ann. Neurol* **70,** 245–254 (2011).
3 Mackay, M. T., Wiznitzer, M., Benedict, S. L., Lee, K. J., Deveber, G. A. & Ganesan, V. Arterial ischemic stroke risk factors: the International Pediatric Stroke Study. *Ann. Neurol.* **69,** 130–140 (2011).
4 Kamada, F., Aoki, Y., Narisawa, A., Abe, Y., Komatsuzaki, S., Kikuchi, A. *et al.* A genome-wide association study identifies *RNF213* as the first Moyamoya disease gene. *J. Hum. Genet.* **56,** 34–40 (2011).
5 Liu, W., Morito, D., Takashima, S., Mineharu, Y., Kobayashi, H., Hitomi, T. *et al.* Identification of *RNF213* as a susceptibility gene for moyamoya disease and its possible role in vascular development. *PLoS ONE* **6,** e22542 (2011).
6 Miyatake, S., Miyake, N., Touho, H., Nishimura-Tadaki, A., Kondo, Y., Okada, I. *et al.* Homozygous c.14576G>A variant of *RNF213* predicts early-onset and severe form of moyamoya disease. *Neurology* **78,** 803–810 (2012).
7 Matsushima, Y., Fukai, N., Tanaka, K., Tsuruoka, S., Inaba, Y., Aoyagi, M. *et al.* A new surgical treatment of moyamoya disease in children: a preliminary report. *Surg. Neurol.* **15,** 313–320 (1981).
8 Karasawa, J., Kikuchi, H., Kawamura, J. & Sakai, T. Intracranial transplantation of the omentum for cerebrovascular moyamoya disease: a two-year follow-up study. *Surg. Neurol.* **14,** 444–449 (1980).
9 Touho, H., Karasawa, J. & Ohnishi, H. Cerebral revascularization using gracilis muscle transplantation for childhood moyamoya disease. *Surg. Neurol.* **43,** 191–197 (1995).
10 Touho, H. Subcutaneous tissue graft including a scalp artery and a relevant vein for the treatment of cerebral ischemia in childhood moyamoya disease. *Surg. Neurol.* **68,** 639–645 (2007).
11 Touho, H., Karasawa, J., Nakagawara, J., Tazawa, T., Yamada, K., Kuriyama, Y. *et al.* Mapping of local cerebral blood flow with stable xenon-enhanced CT and the curve-fitting method of analysis. *Radiology* **168,** 207–212 (1988).
12 Karasawa, J., Kikuchi, H., Furuse, S., Kawamura, J. & Sakaki, T. Treatment of moyamoya disease with STA-MCA anastomosis. *J. Neurosurg.* **49,** 679–688 (1978).
13 Hamada, J. I., Yoshioka, S., Nakahara, T., Marubayashi, T. & Ushio, Y. Clinical features of moyamoya disease in sibling relations under 15 years of age. *Acta. Neurochir.* **140,** 455–458 (1998).
14 Yamauchi, T., Houkin, K., Tada, M. & Abe, H. Familial occurrence of moyamoya disease. *Clin. Neurol. Neurosurg.* **99,** S162–S167 (1997).
15 Wakai, K., Tamakoshi, A., Ikezaki, K., Fukui, M., Kawamura, T., Aoki, R. *et al.* Epidemiological features of moyamoya disease in Japan: findings from a nationwide survey. *Clin. Neurol. Neurosurg.* **99,** S1–S5 (1997).
16 Baba, T., Houkin, K. & Kuroda, S. Novel epidemiological features of moyamoya disease. *J. Neurol. Neurosurg. Psychiatry* **79,** 900–904 (2008).

INTERNAL MEDICINE

□ CASE REPORT □

A Novel *SACS* Mutation in an Atypical Case with Autosomal Recessive Spastic Ataxia of Charlevoix-Saguenay (ARSACS)

Satoko Miyatake[1,2], Noriko Miyake[1], Hiroshi Doi[1], Hirotomo Saitsu[1], Katsuhisa Ogata[2], Mitsuru Kawai[2] and Naomichi Matsumoto[1]

Abstract

Autosomal recessive spastic ataxia of Charlevoix-Saguenay (ARSACS) is an inherited neurodegenerative disorder with symptoms of spastic ataxia, neuropathy, pyramidal sign, finger and foot deformities, and hypermyelination of retinal nerve fibers. *SACS* is mutated in ARSACS. The clinical diversity of ARSACS is recognized, which sometimes makes its diagnosis difficult. By using homozygosity mapping, we identified a novel homozygous c.12020C > T missense mutation in a consanguineous Japanese family with atypical clinical features. In addition to the absence of spasticity and hypermyelinated retinal nerve fibers, the present case had urinary dysfunction, impotence, and severe constipation, indicating the possibility of autonomic dysfunction. Furthermore, we showed the diagnostic usefulness of MRI even for the case of atypical clinical features. It had been considered that cases without obvious spasticity were very rare, however recent reports on atypical cases as well as our case indicate that ARSACS cases without obvious spasticity might be more frequent than previously thought. We should be aware of atypical features of ARSACS for the correct diagnosis.

Key words: ataxia without spasticity, autosomal recessive spastic ataxia of Charlevoix-Saguenay (ARSACS), genetics, homozygosity mapping, *SACS*

(Intern Med 51: 2221-2226, 2012)
(DOI: 10.2169/internalmedicine.51.7374)

Introduction

Autosomal recessive spastic ataxia of Charlevoix-Saguenay (ARSACS: MIM 270550) is an inherited neurodegenerative disorder originally found among French Canadians in the Charlevoix-Saguenay-Lac-Saint-Jean region of Quebec, Canada. The clinical features are early-onset spastic ataxia, nystagmus, axonal and demyelinating neuropathy, pyramidal tract signs, finger and foot deformities, and hypermyelination of retinal nerve fiber. On autopsy, atrophy of the upper vermis and the loss of Purkinje cells in the cerebellum are found. It had been recognized as a highly uniform disease in Quebec (1). In 2000, the gene responsible for ARSACS (*SACS*) was identified (2). *SACS* gene was originally thought to consist of a single giant exon, but eight new coding exons upstream of the gigantic exon were later found (3). Only two causal mutations were found among Quebec patients and a founder effect caused by the settlement patterns from the late 17th to mid-19th century is considered in ARSACS (2, 4). Afterwards, cases with *SACS* mutations were also reported outside Quebec. Now ARSACS is known to exist worldwide (5). Recent reports have also revealed the clinical diversity of ARSACS (6, 7) which sometimes makes its diagnosis difficult.

By homozygosity mapping, we identified a novel homozygous missense mutation in *SACS* in a Japanese family with an atypical clinical phenotype and characteristic MRI findings.

Clinical study

The pedigree is shown in Figure A. Autosomal recessive

[1]Department of Human Genetics, Yokohama City University Graduate School of Medicine, Japan and [2]Department of Neurology, National Hospital Organization Higashi-Saitama Hospital, Japan
Received for publication January 21, 2012; Accepted for publication May 15, 2012
Correspondence to Dr. Naomichi Matsumoto, naomat@yokohama-cu.ac.jp

mode of inheritance was suspected because of the consanguinity. Blood serum test, physiological test such as electrocardiogram, bladder scan to evaluate the postvoid residual urine volume, electrophysiological study including nerve conduction study and somatosensory evoked potential, funduscopic examination of the retina, and MRI study of the brain and spine were performed in addition to the neurological examination.

Genetic study

Blood sample from the proband and the saliva samples from siblings were obtained with informed consent. Genomic DNA was obtained from peripheral blood leukocytes using QuickGene 610-L (FUJIFILM, Tokyo, Japan) and from saliva using Oragene®·DNA (DNA Genotek Inc., Ottawa, Ontario, Canada).

We performed the genome-wide linkage analysis of the consanguineous family with a proband and three unaffected siblings using Affymetrix Human Mapping single nucleotide polymorphism 10K XbaI 142 2.0 array (Affymetrix, Santa Clara, CA, USA). SNP genotyping were undertaken according to the manufacture's protocol. Single nucleotide polymorphism (SNP) allele calls were generated by the GeneChip Genotyping analysis Software (Gtypev4.1). SNP calls and signal detection for the patient and three siblings are 98.73, 96.78, 98.98, 98.65% and 99.81, 99.22, 99.91, 99.86%, respectively. Homozygous mapping was performed using Allegro version 2 based on the autosomal recessive model.

Each of the coding exons and intron-exon border of *SACS*, which was the only known causative gene within the candidate loci, was amplified by PCR using specific primers kindly offered from Dr. Shimazaki (Jichi Medical University School of Medicine) and Dr. Takiyama (University of Yamanashi). PCR products were purified with ExoSAP (USB, Cleveland, OH, USA) and sequenced with BigDye Terminator chemistry version 3 according to the standard protocol (Applied Biosystems, Foster City, CA, USA). The reaction mixture was purified using Sephadex G-50 (GE Healthcare, Buckinghamshire, UK) and multiscreen-96 (Millipore, Billerica, MA, USA). Sequences were obtained on the ABI Genetic Analyzer 3100 (Applied Biosystems) and analyzed with sequence analysis software version 5.1.1 (Applied Biosystems) and Sequencher 4.8-build 3767 (GeneCodes Corporation, Ann Arbor, MI, USA). Experimental protocols were approved by the Committee for Ethical Issue at Yokohama City University School of Medicine.

Case Report

The patient was born under the first-cousin marriage. He started to walk after two years of age. Walking unsteadiness was obvious in his first decade, and was slowly progressive. He needed assistance when walking up stairs in his twenties. He fell frequently because of his unsteady and steppage gait. He was diagnosed as spinocerebellar degeneration when he was 38 years old. He became wheelchair bound at 44 years of age. At that time dysarthria and dysphagia were also observed. He visited our hospital when was 45 years old. On neurological examination at age 54, he had slurred and explosive speech, saccadic eye movement with poor ocular pursuit, dysphagia, cerebellar ataxia in all extremities. Babinski sign was positive. The deep tendon reflexes were diminished or disappeared except for patellar tendon reflex, which was normal. Muscle atrophy and weakness of lower extremities without spasticity was obvious. Position and vibration sense were also decreased in the lower extremities. Interestingly he had urination disorder including pollakiuria, decreased urinary stream, and infrequent urinary incontinence without awareness. He also had impotence, and severe constipation necessitating hospitalization one time. Pes cavus and hammertoe deformity were noticed. He had normal intellectual ability. Hypermyelination of retinal nerve fiber was not observed by funduscopy. Blood sugar, serum beta-lipoproteins, HDL lipoproteins, vitamin E were within normal range. On electrocardiogram (ECG), $CV_{R\text{-}R}$ was normal. The residual urine volume measured with bladder scan just after urination was 83 mL, possibly suggesting urination disorder. It increased to 136 mL a few years later. On nerve conduction study, severe axonal sensori-motor neuropathy with mild demyelinating features was revealed. On SEP study, N20 component of median nerve SEP was delayed, and P38 component of tibial nerve SEP was not evoked (Table 1). MRI findings revealed cerebellar atrophy, especially in the upper vermis, linear pontine hypointensities on T2-weighted imaging, and cervicothoracic spinal atrophy (Figure B).

Molecular findings

We performed homozygosity mapping and identified 10 informative homozygous regions which were larger than 3-Mb in length (Table 2). One of those candidate locus was a 10.3-Mb homozygous region at chromosome 13q11-q12.2 with the maximum LOD score 1.55. Within this region, *SACS* was the only known causative gene for spinocerebellar ataxia. By direct sequencing, novel homozygous c.12020C > T (p.Ser4007Phe) was identified in the patient's sample. Heterozygous c.12020C > T mutation was observed in one of the unaffected siblings, and no mutation in other two unaffected siblings, which was compatible with the haplotype pattern expected from the SNP genotyping, being consistent with the affected status as an autosomal recessive model (Figure A). The amino residue, Ser4007 was evolutionally conserved from anolis to human (Figure C). Four out of 5 computational prediction algorithms (8-11) predicted this mutation to be pathogenic (Table 3). This mutation was not observed in 186 normal Japanese chromosomes.

Discussion

We reported an atypical Japanese case of ARSACS with a novel homozygous missense mutation of the *SACS* gene.

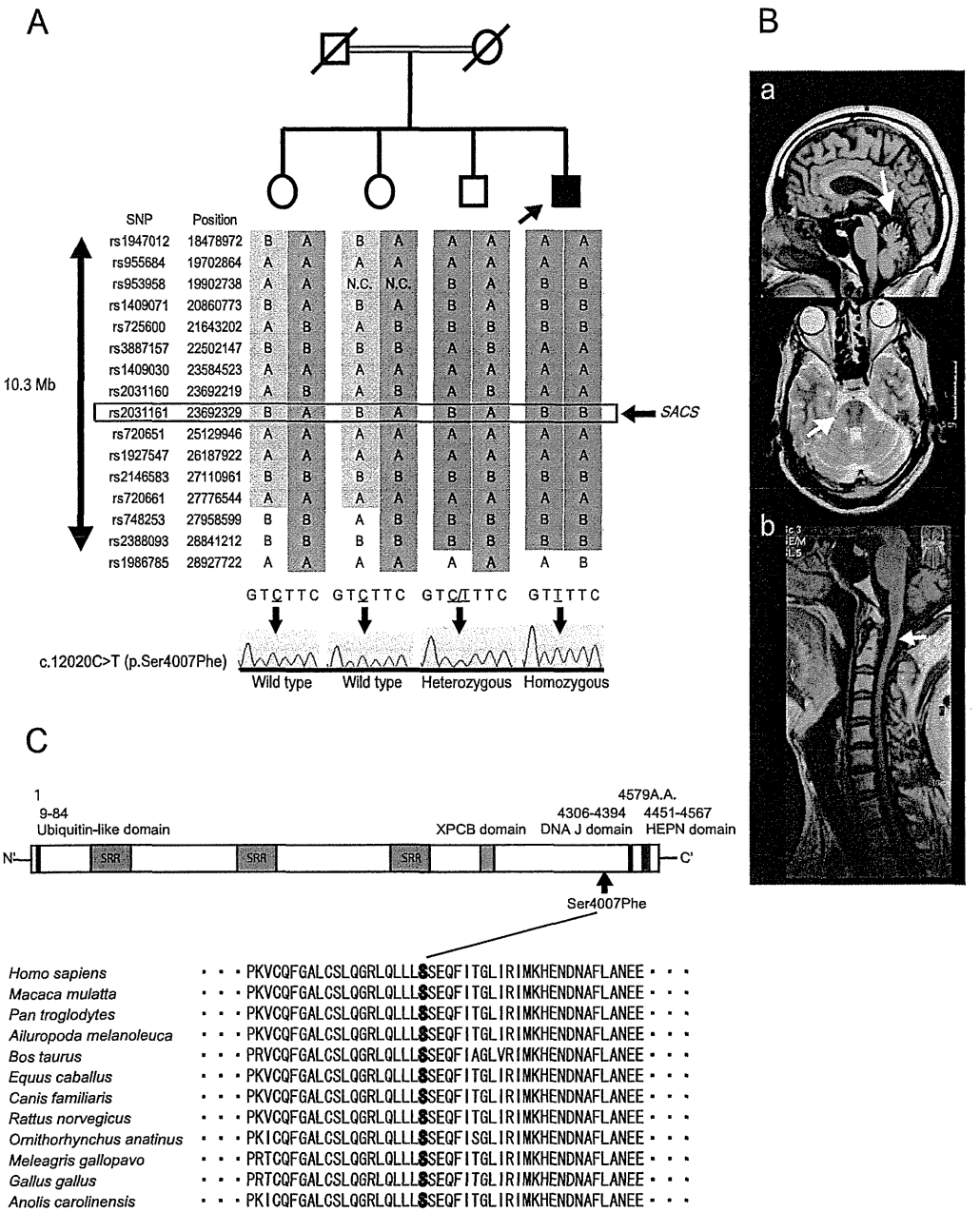

Figure. A. Familial pedigree and haplotypes of the family member at a candidate locus of 13q11-q12.2 identified by 10K SNP microarray. The proband showed a homozygous pattern of the disease allele (shown in blue shadow). The older brother had one disease allele and the other non-disease allele (shown in dark grey shadow) in the heterozygous state. Two older sisters had two different non-disease alleles (shown in dark-grey and light-grey shadows). In the bottom, electropherograms around the c.12020C>T mutation are shown. Proband had a homozygous c.12020C>T mutation. The older brother had a heterozygous c.12020 C>T mutation. Two older sisters show wild-types. These results were compatible with the haplotype pattern, and disease cosegregation. B. MRI of the brain and spinal cord. (a) Brain MRI of the proband showed the atrophy of the cerebellum, especially in the upper vermis in T1-weighted sagittal image (arrow), and linear pontine hypointensities in T2-weighted axial image (arrow). (b) T1-weighted MRI image of the spinal cord revealed cervicothoracic spinal cord atrophy (arrow). C. Sacsin protein with its domains. From the N-terminus to the C-terminus, Sacsin contains several domains: Ubiquitin-like domain, sacsin repeat regions (SRRs), XPCB domain, DNA-J domain, and a higher eukaryotes and prokaryotes nucleotide-binding (HEPN) domain. The mutation newly identified was located upstream of the DNA-J domain and occurred at the highly conserved amino acid.

Table 1. Electrophysiological Study of the Proband

(a) Nerve conduction study

		DL (msec)	Amp	Velocity (m/sec)
Lt. Median N	MCS	4.75	10.4 mV	45.1
	SCS	2.5	0.4 μV	52
Lt. Ulnar N	MCS	2.8	7.4 mV	44.2
	SCS	-	Not evoked	-
Lt. Tibial N	MCS	8.3	0.6 mV	28
Rt. Peroneal N	MCS	6.55	0.06mV	35.6
Rt. Sural N	SCS	-	Not evoked	-

(b) Sensory Evoked Potential study

	EP (msec)	N11 (msec)	N13 (msec)	N20 onset (msec)	N20 peak (msec)
Lt. Median N	not detected	not detected	not detected	33.7	41.7

	P15 (msec)	N20 (msec)	N28 (msec)	P38 onset (msec)	P38 peak (msec)
Lt. Tibial N	not evoked				

DL: Distal latency, Amp: Amplitude, Lt.: Left side, Rt.: Right side, N: Nerve, MCS: Motor conduction study, SCS: Sensory conduction study, EP: Erb's point

Table 2. Candidate Loci Identified by Homozygosity Mapping

chromosomal localization (according to UCSC GRCh37/hg19)	No. of successive homozygous SNPs	Size of homozygous legion (Mb)	Known genes causative for ataxic disorder	maximum LOD score
17q21.2-q23.3	50	23.4		1.55
19q13.12-q13.33	40	12.5		1.55
13q11-q12.2	44	10.3	*SACS*	1.55
3p13-p12.2	17	10.1		1.55
11q13.1-q13.4	4	6.4		1.52
10q11.21-q11.22	14	5.1		1.55
4q34.1-q34.3	22	4.9		1.55
6q22.31-q22.33	17	4.7		1.55
12q23.1	20	4.4		1.54
10p11.22-p11.21	18	4.2		1.55

Notably, spasticity and hypermyelination of retinal nerve fibers which are characteristic features of ARSACS were not observed in this case.

Spasticity is one of the major symptoms of ARSACS inside and outside Quebec. It usually becomes worse as the disease progresses and is prevalent in older patients (1). The cases without obvious spasticity have been considered to be very rare judging from the reviews (6). The cases showing no spasticity were rarely observed, especially in Japanese (12, 13). Recently some additional cases without spasticity have been reported as atypical cases from other ethnic backgrounds, as well as Japanese (14, 15). We should be aware of atypical features in ARSACS for the correct diagnosis. Although spasticity was not obvious in the present patient, ARSACS should not be excluded. The presence of Babinski's sign in spite of distal muscle weakness evident with a history of steppage gait is a strong reminder of pyramidal tract involvement. While the hypermyelination of retinal nerve fibers is a specific finding of ARSACS, this finding is not always observed in patients outside Quebec (16). Another atypical clinical symptom of the present case was urinary dysfunction, impotence, and severe constipation. These symptoms might be due to the pyramidal tract dysfunction, but the progression of urinary dysfunction might indicate the possibility of mild autonomic dysfunction. Urinary urgency/incontinency is occasionally recorded as a symptom of ARSACS. Masciullo et al. have reported an ARSACS case with urinary retention and severe constipation manifesting the intestinal pseudo-obstruction (17). They speculated that the loss of the sacsin protein function leads to the dysfunction of the autonomic ganglia neurons. However their case also had type 1 diabetes which might cause the autonomic dysfunction. Further studies on autonomic function of ARSACS cases will be necessary.

Although the present case had atypical clinical symptoms, MRI findings of this case were quite typical. Early atrophy of superior vermis, and linear hypointensity on T2- and fluid-attenuated inversion recovery (FLAIR)-weighted images of the pons are characteristic of ARSACS (18). We showed here that these MRI findings could indeed help to

Table 3. Computational Prediction of the Novel C.12020 C>T Mutation

Prediction algorithms	Score	Judgment
PolyPhen-2	0.951 (HumVar)	Probably damaging
SIFT	0.11	Tolerated
MutationTaster	4.23	Disease causing
MUpro	-0.03	Decrease the stability of protein structure
Align GVGD	C65	Most likely to interfere with function

PolyPhen-2, SIFT, MutationTaster, MUpro, and Align GVGD are computational prediction algorithms of protein stability changes due to missense mutations. PolyPhen-2 scores close to 1 are likely to be pathogenic. HumVar-trained PolyPhen-2 is a preferred model for diagnosing the Mendelian disease. This prediction was based on PolyPhen-2 v2.0.23r349. SIFT scores less than 0.05 are likely to be pathogenic. In MutationTaster the score is taken from an amino acid substitution matrix, which indicates the degree of difference between the original and the new amino acid considering their physico-chemical characteristics. In MUpro, Support Vector Machine (SVM) scores less than 0 indicate decreases in protein stability. A Grantham variation (GV) and Grantham difference (GD) class more than C55 is likely to be pathogenic in Align GVGD.

diagnose ARSACS, even for patients outside Quebec with atypical clinical features.

SACS encodes the Sacsin protein, a 520 kDa protein expressed highly in neurons, particularly within brain motor system, and cerebellar Purkinje cells (19). Sacsin contains several domains shown in Figure C (20). The c.12020C > T (p.Ser4007Phe) mutation is located upstream of DNA-J domain coding region. Although mutations reported to date spread over entire coding exons or exon-intron border without mutation hotspot, all mutations were detected upstream the DNA-J domain, which was implicated in the chaperone-mediated folding process. Thus it is speculated that ARSACS phenotype might be related to the loss of chaperone function of Sacsin proteinb (16). Further investigation on the function of Sacsin protein is necessary.

It is still obscure whether there is any genotype-phenotype correlation on ARSACS. Takiyama summarized the clinical features of Quebec patients and non-Quebec patients from Japan, Italy, Spain, Tunisia, and Turkey (7). In contrast to the Quebec patients who were clinically uniform with core ARSACS symptoms, non-Quebec patients showed clinical diversities even in its core symptoms. Even most frequent symptoms were different among patients from each country. Ethnic background might modify the ARSACS phenotype, making it complicated to make a correct diagnosis.

The authors state that they have no Conflict of Interest (COI).

Acknowledgement

We thank the patient and his family for their cooperation in this study, Dr. Haruo Shimazaki from Division of Neurology, Department of Internal Medicine, Jichi Medical University School of Medicine, and Dr. Yoshihisa Takiyama from the Department of Neurology, Interdisciplinary Graduate School of Medicine and Engineering, University of Yamanashi, for their offer of the primer sequences.

Grant support: This work was supported by research grants from the Ministry of Health, Labour and Welfare (N. Miyake, H. S. and N. Matsumoto), the Japan Science and Technology Agency (N. Matsumoto), the Strategic Research Program for Brain Sciences (N. Matsumoto) and a Grant-in-Aid for Scientific Research on Innovated Areas-(Foundation of Synapse and Neurocircuit Pathology)-from the Ministry of Education, Culture, Sports, Science and Technology of Japan (N. Matsumoto), a Grant-in-Aid for Scientific Research from Japan Society for the Promotion of Science (N. Matsumoto), a Grant-in-Aid for Young Scientist from Japan Society for the Promotion of Science (N. Miyake and H.S.), a Grant-in-Aid for Japan Foundation for Neuroscience and Mental Health (S.M.).

References

1. Bouchard JP, Barbeau A, Bouchard R, Bouchard RW. Autosomal recessive spastic ataxia of Charlevoix-Saguenay. Can J Neurol Sci **5**: 61-69, 1978.
2. Engert JC, Berube P, Mercier J, et al. ARSACS, a spastic ataxia common in northeastern Quebec, is caused by mutations in a new gene encoding an 11.5-kb ORF. Nat Genet **24**: 120-125, 2000.
3. Ouyang Y, Takiyama Y, Sakoe K, et al. Sacsin-related ataxia (ARSACS): expanding the genotype upstream from the gigantic exon. Neurology **66**: 1103-1104, 2006.
4. Laberge AM, Michaud J, Richter A, et al. Population history and its impact on medical genetics in Quebec. Clin Genet **68**: 287-301, 2005.
5. Gomez CM. ARSACS goes global. Neurology **62**: 10-11, 2004.
6. Bouhlal Y, Amouri R, El Euch-Fayeche G, Hentati F. Autosomal recessive spastic ataxia of Charlevoix-Saguenay: an overview. Parkinsonism Relat Disord **17**: 418-422, 2011.
7. Takiyama Y. Sacsinopathies: sacsin-related ataxia. Cerebellum **28**: 1-7, 2007.
8. Adzhubei IA, Schmidt S, Peshkin L, et al. A method and server for predicting damaging missense mutations. Nat Methods **7**: 248-249, 2010.
9. Ng PC, Henikoff S. Predicting deleterious amino acid substitutions. Genome Res **11**: 863-874, 2001.
10. Cheng J, Randall A, Baldi P. Prediction of protein stability changes for single-site mutations using support vector machines. Proteins **62**: 1125-1132, 2006.

11. Mathe E, Olivier M, Kato S, et al. Computational approaches for predicting the biological effect of p53 missense mutations: a comparison of three sequence analysis based methods. Nucleic Acids Res **34**: 1317-1325, 2006.

12. Shimazaki H, Takiyama Y, Sakoe K, Ando Y, Nakano I. A phenotype without spasticity in sacsin-related ataxia. Neurology **64**: 2129-2131, 2005.

13. Shimazaki H, Sakoe K, Niijima K, Nakano I, Takiyama Y. An unusual case of a spasticity-lacking phenotype with a novel *SACS* mutation. J Neurol Sci **255**: 87-89, 2007.

14. Baets J, Deconinck T, Smets K, et al. Mutations in *SACS* cause atypical and late-onset forms of ARSACS. Neurology **75**: 1181-1188, 2010.

15. Shimazaki H, Takiyama Y, Honda J, et al. Middle cerebellar peduncles and pontine T2 hypointensities in ARSACS. J Neuroimaging 2012 [Epub ahead of print].

16. Bouhlal Y, Amouri R, El Euch-Fayeche G, Hentati F. Autosomal recessive spastic ataxia of Charlevoix-Saguenay: an overview. Parkinsonism Relat Disord **17**: 418-422, 2011.

17. Masciullo M, Modoni A, Fattori F, et al. A novel mutation in the *SACS* gene associated with a complicated form of spastic ataxia. J Neurol **255**: 1429-1431, 2008.

18. Martin MH, Bouchard JP, Sylvain M, St-Onge O, Truchon S. Autosomal recessive spastic ataxia of Charlevoix-Saguenay: a report of MR imaging in 5 patients. AJNR Am J Neuroradiol **28**: 1606-1608, 2007.

19. Parfitt DA, Michael GJ, Vermeulen EG, et al. The ataxia protein sacsin is a functional co-chaperone that protects against polyglutamine-expanded ataxin-1. Hum Mol Genet **18**: 1556-1565, 2009.

20. Kozlov G, Denisov AY, Girard M, et al. Structural basis of defects in the sacsin HEPN domain responsible for autosomal recessive spastic ataxia of Charlevoix-Saguenay (ARSACS). J Biol Chem **286**: 20407-20412, 2011.